https://doi.org/10.5194/egusphere-2026-3226
Preprint. Discussion started: 22 July 2026

A stochastic model of hierarchical sediment transport in watershed

Jun Zhang[a, b], Yong Li[a*], Xiaojun Guo[a], Dongri Song[a], Jens M. Turowski[c]

[a] Key Laboratory of Mountain Hazards and Engineering Resilience/Institute of Mountain Hazards and Environment, Chinese Academy of Sciences, Chengdu 610041, China

[b] State Key Laboratory of Hydroscience and Engineering, Department of Hydraulic Engineering, Tsinghua University, Beijing 100084, China

[c] German Research Centre for Geosciences (GFZ), Telegrafenberg, 14473 Potsdam, Germany

*Corresponding author: Yong Li, ylie@imde.ac.cn

Abstract: Debris flows often occur as intermittent surges in succession; a single event may comprise tens to hundreds of separate surges. While previous studies have focused primarily on isolated surge dynamics, the temporal evolution and statistical properties of the surge sequences as an entirety remain poorly understood. Here, we present a comprehensive analysis of global debris flow datasets, including velocity, discharge, sediment volume, and inter-surge intervals. We quantitatively characterize the surge sequences by the statistic features of the key parameters, revealing 1) a general decay trend in fluctuating discharge, 2) universal distributions for flow velocity (Weibull), discharge/sediment volume (exponentially-modified power-law), and inter-surge intervals (exponential), and 3) self-similar structure in sequence organization. These findings motivate the development of a novel stochastic modeling framework that conceptualizes surge sequences through three key components: 1) The cascading thinning of mass sequences originating from Poisson processes of source failures and inter-processes of bank and bed erosions driven by hydrologic process, 2) a selection coefficient generated through Gaussian process to integrate the effective contributions of mass from multi-sources, 3) model parameter calibration using local monitoring data and experimental validation. Numerical simulations demonstrate the model's ability to accurately replicate observed surge sequences. Notably, the framework spontaneously generates a unified distribution of discharge and sediment volume in the form of a truncated power-law with an exponential cutoff. This provides a novel magnitude–frequency relationship for mass movements

https://doi.org/10.5194/egusphere-2026-3226
Preprint. Discussion started: 22 July 2026

and can also be applied to large-scale sediment transport studies.

Key words: debris flow; surge sequence; probability distribution; stochastic model; temporal variation

1. Introduction

Sediment transport in river basins operates as a hierarchical cascade (Fryirs et al., 2013), with debris flows representing a typical manifestation of this process (Iverson, 1997a; Takahashi, 2007). Debris flows often propagate as surge waves, with many events consisting of multiple successive surges that exhibit significant variability in magnitude and dynamics (Arai et al., 2013; Arattano, 1999; Forterre & Pouliquen, 2003). To date, monitoring systems have systematically captured the characteristics of debris flow surges across various conditions and watersheds worldwide (Hürlimann et al., 2019). Debris flows originate primarily through two distinct mechanisms: the mobilization of landslides (often referred to as landslide-initiated debris flows) (Iverson et al., 1997), and the progressive erosion and bulking of channel bed and banks by surface runoff (runoff-generated debris flows) (Coe et al., 2008; Simoni et al., 2020). During propagation, sediment entrainment and hydraulic erosion can further amplify the flow mass (Hungr et al., 2014; Pudasaini, 2012; Takahashi, 2007). The emergence of successive surges is governed by two mechanisms: the roll wave kinetics from flow instability (Forterre and Pouliquen, 2003), as observed in both natural phenomena and laboratory studies; and discontinuous supplies of mass from spatially distributed sources, such as punctual bank erosion, slope failures, and dam-failure cycles in streams (Coe et al., 2008; Davies, 1992; Gregoretti and Fontana, 2008; Kean et al., 2011, 2013; Zanuttigh & Lamberti, 2004, 2007). Consequently, research has mainly focused on individual surges, particularly their formation mechanisms, dynamic characteristics, frontal geometry, longitudinal flow variations, peak discharge amplification, and sediment erosion-transport-deposition processes (e.g., Hungr, 2014; Nagl et al., 2024; Pudasaini, 2012; Takahashi, 2007; Trujillo-Vela et al., 2022). However, understanding individual surges does not necessarily facilitate the identification of successive surge occurrences. This limitation stems from the scarcity of long surge series at routinely monitored sites,

https://doi.org/10.5194/egusphere-2026-3226
Preprint. Discussion started: 22 July 2026

where >83% of instrumented catchments record events with <20 surges (Hürlimann et al., 2019) — despite exceptional cases like Jiangjia Gully (JJG), China, exhibiting tens to hundreds of surges—which renders sequential patterns statistically insignificant for robust analysis (Cui et al., 2005; Davies, 1992; Iverson, 1997a; Liu et al., 2009; Takahashi, 2007; Yang et al., 2019).

Typical surge sequences demonstrate remarkable diversity in flow regimes, spanning from laminar to turbulent states, and are accompanied by noteworthy variability in key parameters such as bulk density (1.4-2.4 g/cm^3), discharge (10-10^3 m^3/s), and sediment volume (10^2-10^5 m^3) (Liu et al., 2009; Yang et al., 2019). Despite these observable features, a comprehensive quantitative explanation remains elusive. For instance, the number of surges per event, the reasons behind the magnitude variations spanning multiple orders of magnitude, and the probabilistic distributions of key variables (e.g., discharge and velocity) remain unclear. We propose that surge sequences act as integrated systems encoding the full evolving processes from source materials to channelized flow. Particularly, the variations in surge features reflect underlying generation mechanisms: fluctuations in density correspond to heterogeneity in source materials, while variability in discharge arises from interactions between processes operating across multiple scales. Notably, despite their diverse origins, surge sequences exhibit universal statistical patterns, including magnitude decay trends, Weibull-distributed velocities, and exponentially distributed discharges and inter-surge intervals (Liu et al., 2009; Yong et al., 2012, 2013). These consistent features strongly suggest the existence of overarching physical principles governing surge generation, thus highlighting the need of a unified modeling framework.

Surge phenomena pose a fundamental challenge in debris flow prediction due to their inherently discontinuous nature. Current dynamic models generally assume continuous mass movement using hydrological and hydrodynamic models under prescribed rainfall and soil saturation conditions. They simulate debris flows as a single continuous process and predict a single flow of certain magnitude; but they do not predict discrete surges with highly fluctuating peak discharges and variation patterns in sequences. This limitation arises because the underlying structure of many dynamical models, often conceptualized as a cascade of hydrological, entrainment, and hydraulic components, struggles to fully represent the diverse and discontinuous initiation mechanisms and supply processes of debris flows observed in nature (Baggio et al., 2021; Gregoretti et al., 2019; Hungr et al., 2014; Iverson, 2014; Liu et al., 2020).

This study aims to develop a universal stochastic framework to model the formation and evolution of debris flow surges and generate the surge sequences, with three primary objectives: (1) to statistically characterize surge sequences, (2) to predict the forming and developing of successive surges, and (3) to uncover the underlying physical mechanisms of mass transport in watershed. To achieve these objectives, we propose a methodology that integrates three key components: (i) a comprehensive analysis of temporal characteristics of surge sequences using monitoring dataset in JJG; (ii) the development of a stochastic framework incorporating Poisson process of slope failures in source areas, and (iii) cross-watershed validation through comparative analysis of surge sequences from diverse geological settings. The manuscript is organized as follows. First, in the section on data synthesis and statistical characterization, we compile a global dataset of surge events, provide detailed parameterization for the JJG case, and identify the probability distributions of key variables. Next, we present the model formulation, which involves the development of a stochastic surge generator that couples slope failures in the source area with sediment transport through a hierarchical watershed structure. This is followed by model evaluation, where we quantitatively assess the model performance using JJG benchmarks and demonstrate its applicability to other contrasting watersheds over the world. Finally, we discuss the broader implications of the proposed framework for debris flow forecasting and its potential utility in debris flow dynamics and general sediment transport processes.

2. Data Sources, Measurements, and Statistical Methods

2.1 Data Source from Global Watersheds

This study utilizes two primary debris-flow datasets: (1) a dataset from JJG, employed for the statistical analysis of surge sequences (Section 2.3), model development (Section 3.1 and 3.2) and subsequent verification (Section 4); and (2) a dataset from multiple global watersheds, used for model validation (Section 4.2.1 and 4.2.2).

JJG (detailed description is provided in Test S1 of the Supporting Information) typically exhibit

https://doi.org/10.5194/egusphere-2026-3226
Preprint. Discussion started: 22 July 2026

multi-surge characteristics, with event sequences consisting of tens to hundreds of surges. The JJG dataset comprises more than 400 debris flow events, including nearly 10,000 individual surges; and for each surge, the following parameters are documented: flow depth (h, m, typically representing surge front height), velocity (v, m/s), discharge (Q, m^3/s), flow density (ρ, kg/m^3), volumetric solid concentration (C_s), sediment delivery (S, m^3), and the time interval (τ, s) between successive surge fronts (Hong et al., 2015; Hu et al., 2011; Li et al., 2015). This dataset is publicly available through the Dongchuan Debris Flow Observation and Research Station of the Chinese Academy of Sciences (DDFORS, https://doi.org/10.12380/Debri.msdc.000027).

To evaluate the universality of the statistical characteristics of debris-flow parameters and to verify the reliability of the proposed model, additional datasets from 12 representative global watersheds were analyzed. These include Kamikamihorizawa Creek (Japan), Sleeping Child Creek (USA), Chalk Cliffs (USA), and Gadria Creek (Switzerland) (Figure 1b). Detailed topographic characteristics and monitoring periods for each watershed are provided in Text S2 of the Supporting Information.

2.2 Field Measurements in JJG

Individual surges are characterized by a turbulent front enriched with coarse grains, followed by a high-concentration flow body and a shallow tail composed predominantly of fine-grained slurry (Figure 1b-4, 5). Measurements were conducted on surge fronts using the following procedures, incorporating strict quality control protocols (e.g., sensor calibration, standardized sampling, multiple independent observers for timing to reduce error):

(1) Flow depth (*h*): Continuously recorded at 10 Hz using an ultrasonic sensor (± 0.1% accuracy) suspended 6.0 m above the channel centerline (Du et al., 2023).

(2) Velocity (*v*): Calculated as $v=\Delta L/\Delta t$, where ΔL is the fixed distance (200 m) between two monitoring cross-sections (Fig. 1b-7), measured using electronic distance measurement (accuracy: 0.6 mm + 1 ppm). The travel time Δt for the surge front between sections was recorded using high-precision stopwatches (resolution: 5 μs; accuracy: ±1 ppm).

(3) Discharge (*Q*): Calculated as $Q = vWh$, where W is the channel width at the measurement section, determined using a measuring tape (Hong et al., 2015).

https://doi.org/10.5194/egusphere-2026-3226
Preprint. Discussion started: 22 July 2026

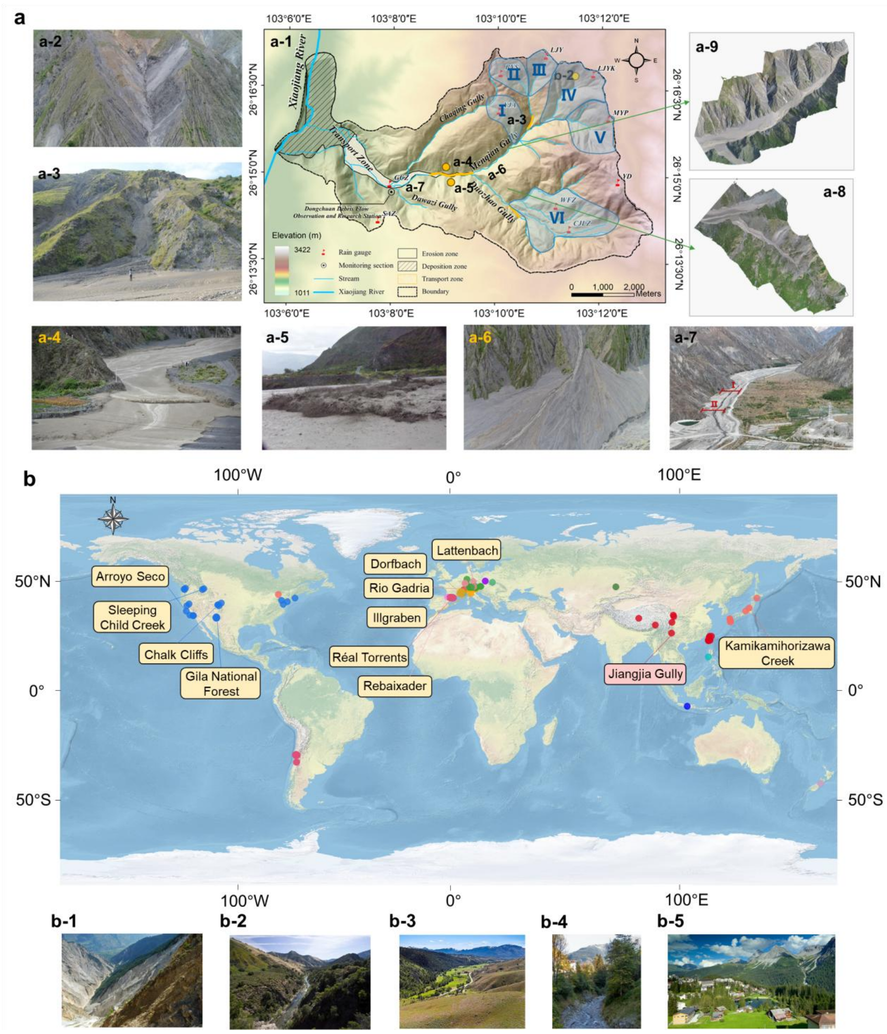

Figure 1. Data sources of worldwide debris flow catchments in this study. (a) Debris flow observations in Jiangjia Gully, China. (a-1) Overview of JJG and source areas, including rainfall gauges: YJA (I), BYS (II), LJY(III), LJYK (IV), MYP (V), WFZ and CJLZ (VI); (a-2) Morphology of a representative source area; (a-3) Source slopes and a tributary; (a-4) Successive surges in the mainstream channel; (a-5) Turbulent surge front; (a-6) Deposits in a tributary outlet; (a-7) JJG observation station with monitoring cross-sections (I and II) used for determining surge velocity and arrival time, enabling calculation of inter-surge intervals; (a-8, a-9) UAV-derived Digital Elevation Models (DEM) of the two major tributaries. (b) Locations of debris flow sites across 12 catchments. (b-1) Illgraben, Switzerland (Bolliger et al., 2024); (b-2) Arroyo Seco, USA (Cannon, 2003; Kean

https://doi.org/10.5194/egusphere-2026-3226
Preprint. Discussion started: 22 July 2026

et al., 2011); (b-3) Sleeping Child Creek, USA (McCoy et al., 2012); (b-4, b-5) Lattenbach, Austria and Dorfbach, Switzerland (Mitchell et al, 2022).

(4) Flow density (ρ) and solid concentration (C_s): Slurry samples were collected from the flow body using a sampling pole and cylindrical containers. Flow density ρ was computed from the mass-to-volume ratio. Multiple samples (typically 3-5) were taken per major surge, and the reported values for ρ and C_s represent per-surge averages. Volumetric solid concentration was calculated as $C_s=(\rho-\rho_w)/(\rho_s-\rho_w)$, where water density ρ_w = 1,000 kg/m^3 and solid grain density ρ_s = 2,650 kg/m^3 (Du et al., 2023).

(5) Sediment delivery (S): Volume of solid material per surge. It was estimated using $S = (\rho C_s Q_{avg})T$, where ρ, C_s, and Q_{avg} are the per-surge average flow density, volumetric solid concentration, and discharge, respectively. Q_{avg} was calculated as the arithmetic mean of instantaneous Q over the surge duration T, both derived from the continuous flow depth record (Takahashi, 1991).

(6) Time interval (τ): The time interval is defined as the time difference between two successive surge fronts passing the observing cross-section, which is recorded using redundant chronometer to ensure accuracy and reliability (Wei et al., 2025).

For the present purpose of understanding the sequential features of the surges, we consider the key properties: v, Q, S, and τ, representing the velocity, flow rate, total volume (hence the duration), and intermittency of the surges. Multiple sequences with complete data of the measured properties were utilized to analyze sequential patterns and statistical characteristics. The dataset spans from the 1980s to the present and covers a wide range of flow regimes, making it representative of typical surge behavior in JJG. It thus provides a sound physical basis for model development, while data from other watersheds are employed for model verification and generalization.

2.3 Methods for Data Analysis

As the objective is to capture the properties of the surge sequence, we consider the statistical features of the measured data, i.e., the temporal pattern of the sequence and the probability distribution of the variables. For this, the following methods are employed.

https://doi.org/10.5194/egusphere-2026-3226
Preprint. Discussion started: 22 July 2026

(1) Moving Average of Discharge and Sediment Delivery

We define the moving average of quantity X as

$$\langle X\rangle_n = (x_1 + x_2 + \cdots + x_n)/n, \qquad n = 1, 2, ..., N \tag{1}$$

to feature the overall trend of the significant fluctuations. Here we consider X as the discharge Q and sediment volume S, $\langle\cdot\rangle$ represents the averaging operator, and n is the number of surges included in the average. This defines a temporal function $\langle X\rangle_n = f(n)$ to describe the average fluctuation of the surges, noting that the progressing n can be substituted by the corresponding time of the surge. It proves that the surge sequences appear to have a decaying $f(n)$, varying in power-law form with the process: $f(n) \sim n^{-q}$.

(2) Probability Distributions

Probability distributions characterize the frequency of occurrence of a variable within a sequence. The measured quantities (v, Q, S, τ) are found to follow specific probability distributions.

***v* Distribution:** The distribution of flow velocity is observed to follow a Weibull distribution (Yong et al., 2012):

$$p(v) = (k/\eta)(v/\eta)^{k-1}\exp(-(v/\eta)^k) \tag{2}$$

where the scale parameter η is estimated by the sample mean, and the shape parameter k is estimated using Maximum Likelihood Estimation (MLE) (Stone et al., 2007). Alternatively, one may use the distribution function, $P(<v) = 1 - \exp(-(v/\eta)^k)$, showing the percentage of surges exceeding velocity v. For comparing different events, we may rescale $v^* = \langle v^2\rangle/\langle v\rangle$ and obtain a unique curve $P(v^*)$.

***Q* and *S* Distribution:** Surge magnitude is represented by discharge and sediment volume, Q and S. We'll find that both satisfy a power-law distribution modified by an exponential function:

$$P(M) = CM^{-\mu}\exp(-M/M_c) \tag{3}$$

where $P(M)$ is the exceedance percentage, and C, μ, and M_c are fitting parameters. Since C is a normalization constant, the distribution reduces to the parameters μ and M_c. Furthermore, it can be reduced to an exponential function

$$P^*(M) = \exp(-M^*) \tag{4}$$

when M is rescaled by M/M_c, and $P(M)$ is rescaled by $P^*(M) = PM^{\mu}/C$. This means that the

https://doi.org/10.5194/egusphere-2026-3226
Preprint. Discussion started: 22 July 2026

distributions for various events must collapse upon a unique exponential curve.

***τ* Distribution:** The distribution of time intervals between successive surges is found to follow an exponential distribution:

$$P(\tau) = (1/\lambda)\exp(-\lambda\tau) \quad (5)$$

where $P(\tau)$ is the exceedance percentage of τ, and λ is the exponent defining the characteristic time $\tau_c = 1/\lambda$. This distribution is actually the necessary and sufficient condition for identifying the surge sequence as a Poisson process. Again, it can be further rescaled as

$$P^*(\tau) = \exp(-\tau^*) \quad (6)$$

where $\tau^* = \tau/\langle\tau\rangle$ and $P^*(\tau) = P(\tau)/\lambda$.

The converge of distributions for different events provides an intuitive confirmation to the distributions, and this further indicates that these diverse sequences share identical statistical characteristics.

3 Model Formulation Based on Statistical Characteristics of Surge Sequences

3.1 Fluctuation and Variability of Surge Sequences in JJG

Debris flow surges in JJG exhibit a highly unsteady nature, which reflects the universal characteristics of surge sequences observed globally. Field measurements of (v, Q, S, τ) reveal significant fluctuations: $v\in(0.2, 14.4)$, $Q\in(0.4, 2262)$, $S\in(12.6, 3280)$, and $\tau\in(10, 1000)$ (in the units mentioned above). Figure 2 presents the fluctuations for the sequences of two events, E910709 and E000704, which occurred on July 9, 1991, and July 4, 2000, respectively. These represent the long-duration (427 surges) and short-duration (75 surges) events.

Among these quantities, the variation in flow density holds special significance regarding the origin of surges, due to its correlation with the grain size distribution (GSD) of the sediment. Specifically, ρ increases with P(>2mm), the proportion of coarse grains, while decreases with P(<0.05mm), the proportion of fine grains (Fig. 2c). Here, the boundary sizes distinguishing coarse and fine grains are chosen somewhat arbitrarily; however, other boundary sizes also work effectively in this context. Generally, one finds power-law ρ-GSD relationships for debris flows

(Wang et al., 2018; Yang et al., 2019), which suggests that the surge flow has dynamically regulated the GSD of the sediment materials. This is further reflected by the fact that high-ρ surges (up to 2.30 g/cm³) are characterized by high-Q, high-v (v > 5 m/s), and high-frequency or short-τ ($\tau \approx$ 100s); while low-ρ surges (down to 1.4 g/cm³) are characterized by low-Q, low-v (v < 4 m/s), and low-frequency or long-τ (τ > 1000 s).

Accordingly, ρ-variation serves both as an indicator of source material heterogeneity and as a dynamic proxy for underlying flow evolution mechanisms. Furthermore, the covariation patterns of the observables provide essential constraints for the modeling of surge dynamics. This forms the basis of our model framework.

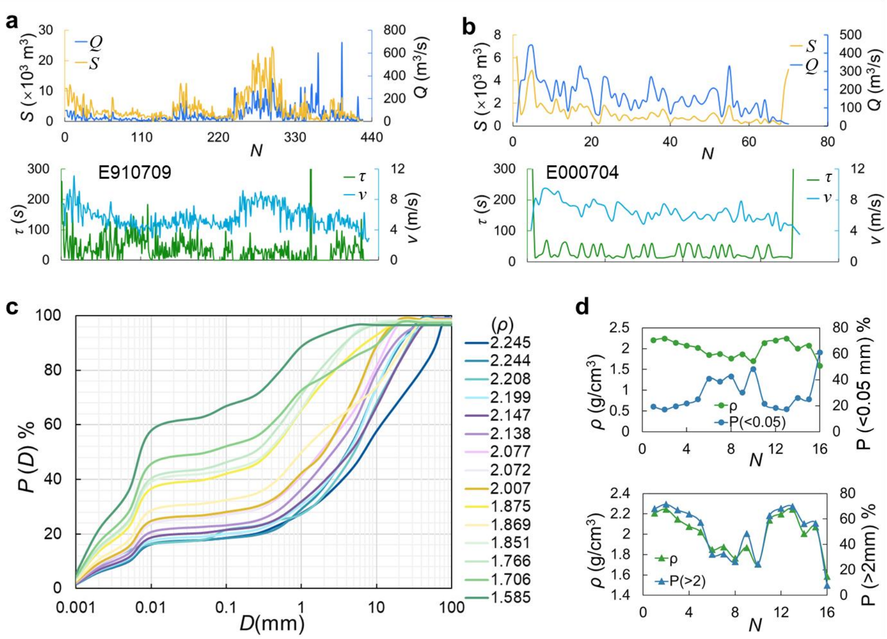

Figure 2. Fluctuations of surge sequences for two debris-flow events (E910709 and E000704). (a) and (b): Fluctuations of the observed properties (Q, S, v, τ); (c) Cumulative GSD curves (P(>D)%) for surges with different densities (ρ). (d) Variation of ρ with GSD, showing decrease with fine content P (< 0.05mm) and increase with coarse content P(> 2mm).

3.2 Universal Statistical Characteristics of Surge Sequences

https://doi.org/10.5194/egusphere-2026-3226
Preprint. Discussion started: 22 July 2026

Applying the methods outlined in Section 2.3, we can quantify both the overall fluctuation trends and the probability distributions of the observed variables. The features of surge sequences across different events are consistent, including the decay trend of discharge (Fig. 3a-2), the probability distributions of Q, S, v, and τ (Fig. 3a-3,4,5), and the similarity between surge groups within a single event (Fig. 3b).

(1) General decaying trend of discharge

The surge sequences exhibit a general decaying trend, characterized by the moving average $<Q>_n \sim n^{-q}$, with q ranging from 0.24 to 0.98. The turning point, N_t, appears randomly within the sequence (Fig. 3a-2). This behavior contrasts markedly with white noise sequences, which inherently converge toward a steady-state condition characterized by $q = 0$. For instance, we find that in many hydrographic processes in great rivers (e.g., the Yellow River), the fluctuation of flood discharge presents like a white noise series ($H \sim 0$), with decaying exponent $q \sim 0$. Therefore, the observed power-law decaying indicates significant inter-surge correlations between surges, consistent with the Hurst exponent ($H \approx 0.90$) reported for most sequences (e.g., Zhang et al., 2021). In other words, such a decaying trend reflects the auto-correlation of the surge sequences. In fact, data in JJG shows that the sequences are long-rang correlation in that the auto-correlation coefficient obeys a power-law decay, $C_{auto}(n) \sim n^{-\beta}$, with exponent β between (0.35, 0.69), and the correlated range n varies from 0.10 to 0.70N, N being the total number of surges.

(2) Modified power-law distribution of magnitude

The surge magnitude is characterized by discharge (Q) and sediment volume (S), both of which follow a unified distribution expressed as a power-law distribution modified by an exponential function (Eq. 3). The rescaled curve $P^*(M) = \exp(-M^*)$ fits the events perfectly (Fig. 4a-3), demonstrating the robustness and consistency of the distribution.

While power-law distributions are common in natural phenomena such as landslides, floods, and earthquakes (Bowers et al., 2012; Graber et al., 2022; Hergarten, 2002), the exponential modification suggests distinct underlying mechanism for its emergence. This hybrid distribution represents a novel pattern in geophysical flows that demands new physical interpretation.

(3) Weibull distribution of velocity

https://doi.org/10.5194/egusphere-2026-3226
Preprint. Discussion started: 22 July 2026

The Weibull distribution of surge velocity (Eq. 2) shows a constant scale parameter η (6.41 on average) and shape parameter α that varies depending on events. This yields an average velocity of $\langle v\rangle=\eta\Gamma(1+1/\alpha) \sim 0.90\eta$, and a probability for characteristic velocity (i.e., $v=\eta$), $P(>\eta) = e^{-1} \approx 0.37$. Consequently, more than 63% of surges exhibit velocities below the mean value, which is consistent with our observed proportion of approximately 60%.

Related to the velocity is the Froude number, $Fr=v/(gh)^{1/2}$, which quantifies the relative influence of gravity and inertia, thereby determining the flow state. Here h is the flow depth (average of the measurements) and g the gravitation acceleration (9.81 m/s^2). We consider Fr in the context because of its correlation to the potential mechanism of surge emergence. Most surges in JJG are found to be in supercritical state (i.e., $Fr > 1.0$) (Du et al., 2023), implying that they are dominated by inertia due to high concentration of sediment (C_s). When surge is considered as roll waves, Fr serves as a critical indicator of flow instability (Arai et al., 2013; Ng & Mei, 1994). However, the high C_s may significantly modify the critical Fr for onset of roll wave (or flow instability), particularly in the gentle channel of slope less than several degrees (<5° in the mainstream channel of JJG). Additionally, the substantial variation in C_s and sediment composition suggest that surges do not originate from a single common source flow.

(4) Exponential distribution of inter-surge time interval

The exponential distribution of inter-surge time interval (Eq. 6, Fig. 3a-5) is particularly significant because it serves as both the necessary and sufficient condition for identifying the Poisson process (Krishnan, 2015; Lari et al., 2014). Our results therefore indicate that surges constitute a Poisson process, representing the most fundamental class of stochastic point processes.

As observed above (Fig. 2a and 2b), high-ρ surges tend to occur in clustered groups with relatively short intervening intervals. This pattern manifests as large λ values, indicating intense surge activity where major events occur in rapid succession. The parameter λ thus provides a characteristic measure that simultaneously captures two key aspects of the debris flow process: the inherent discontinuity between individual surges and the persistent nature of the overall process.

(5) Self-similarity of surge sequence

A long surge-sequence event typically consists of multiple sub-events. For example, the

https://doi.org/10.5194/egusphere-2026-3226
Preprint. Discussion started: 22 July 2026

E910709 sequence with 427 surges appears to comprise of four distinct surge groups, labeled A, B, C, and D (Fig. 3b-1). Each group is identified by the surges with discharge dropping to near zero. These surges might result from the discontinuity of mass supplies or erosion-deposition waves (Edwards et al., 2021; Viroulet et al., 2019). Data analysis confirms that each group behaves as an independent event exhibiting similar characteristics: the consistent decaying trends (Fig. 3b-2) and the similarity in probability distributions for surge magnitude (Fig. 3b-3), velocity (Fig. 3b-4), and inter-surge time intervals (Fig. 3b-5).

https://doi.org/10.5194/egusphere-2026-3226
Preprint. Discussion started: 22 July 2026

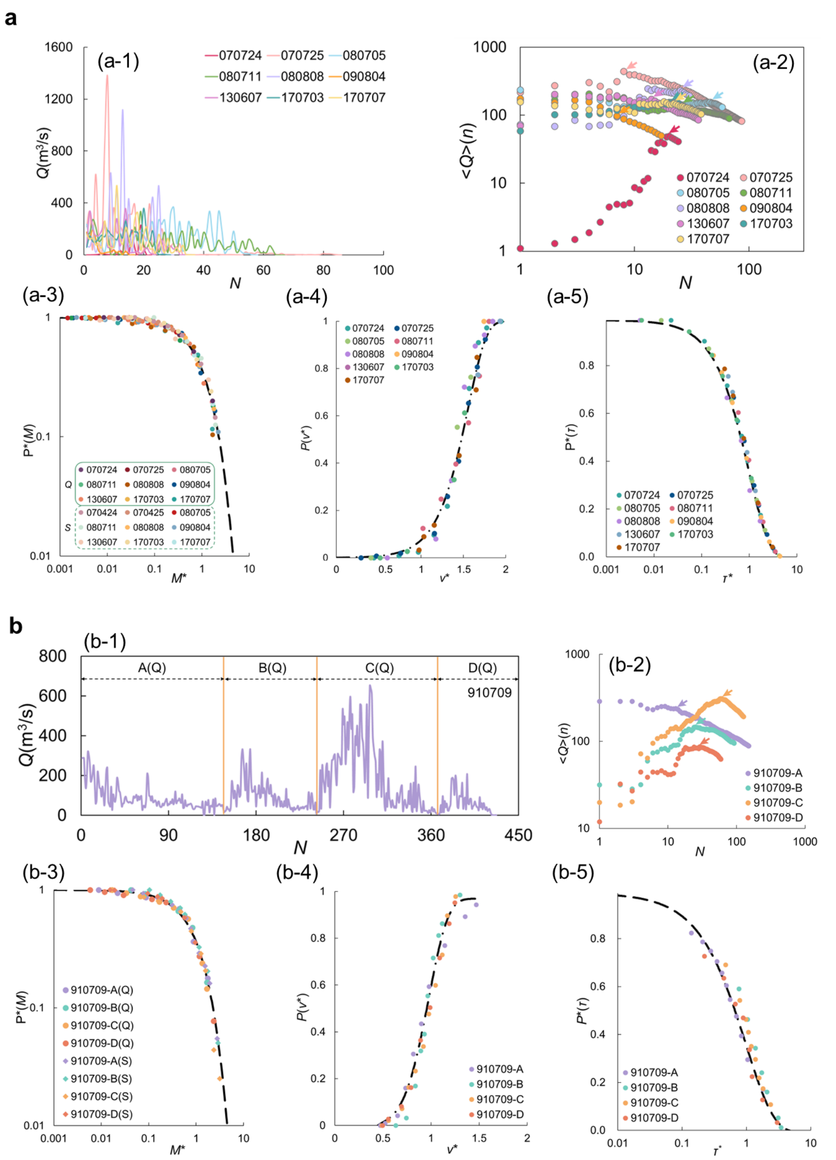

Figure 3. Statistical characteristics of surge sequences in JJG (a) and a single event consisting of several sub-sequences (E910709) (b). (a-1) Q-fluctuation of surge sequences for nine events; (a-2) Overall decay trend of discharge with a power-law tail, $\langle Q\rangle_n \sim n^{-q}$; (a-3) Unified scaling distribution for Q and S (denoted by M in the plot); (a-4) Weibull distribution of flow velocity; (a-5) Exponential distribution of inter-surge time intervals. (b-1) Q-fluctuation of surges in four groups, with each group (sub-sequence) exhibiting consistency in (b-2) Overall trend of Q with power-law tail; (b-3) Scaling distribution for Q and S (M); (b-4) Weibull distribution of velocity; and (b-5) Exponential

https://doi.org/10.5194/egusphere-2026-3226
Preprint. Discussion started: 22 July 2026

distribution of inter-surge time interval.

In summary, the statistical features of surge sequences provide valuable insights into their emergence, especially the following key characteristics:

(1) Multi-source origins and complex confluence

The wide range of observed fluctuations in flow density and discharge suggests the multi-source origins of the surges. The complex flow composition that is more consistent with the incorporation of materials and flow interactions during transport than with simple roll wave instability (Iverson et al., 2005). The relationship between ρ and textural fraction of sediment highlights the dynamic sorting and segregation processes within the surge flow, which govern the distinct characteristics of high- and low-magnitude surges (Zhou et al., 2019).

(2) Limited mass supplies and sediment entrainment

The consistent decay trend in moving average discharge ($\langle Q \rangle_n$) is consistent with the fact that sediment supplies from slope failures in source areas and bank erosions are intermittent and limited during the event even with ongoing rainfall (Guo et al., 2021); additionally, this indicates that the flow has a restricted capacity to transport sediment. In a single surge, the flow assimilates sediments concentrated on the front while leaving a progressively finer and muddy tail (Iverson et al., 2005; Zhou et al., 2019).

(3) Stochastic timing

Debris-flow events lack a definitive start or end time. Mass supplies are randomly distributed in both space and time, and individual surges have no identifiable source. The only observable temporal aspects of a surge are its arrival time at a specific location and the intervals between consecutive surges. The exponential distribution of these inter-surge intervals indicates that surges can be modeled as a Poisson process (Krishnan, 2015).

(4) Scale-invariant magnitude distribution

The modified power-law distribution of discharge (Q) and sediment volume (S) (Eq. 2 and 3) establishes a novel magnitude-frequency relationship with scale-invariance. Comparing with the power-law distribution that describes the heavy tail with a roll over in small events, as in the case

https://doi.org/10.5194/egusphere-2026-3226
Preprint. Discussion started: 22 July 2026

of earthquakes and landslides, the new distribution fits the data perfectly over the entire range, as illustrated by the curves (Fig. 3, 6, 7, 8). Power laws have been associated with self-organized criticality (Marković & Gros, 2014), whereas this modified distribution calls for a new interpretation, especially in the context of debris flows.

(5) Self-similar structure of sequence

The self-similarity observed within a surge sequence implies a common developmental pattern in individual surges, characterized by the superposition of materials derived from multiple sources. Importantly, this similarity between subsequences and the overall sequence also indicates that properties identified in longer sequences are applicable to shorter sequences, which often lack sufficient data for robust statistical analysis.

A comprehensive debris flow model should be capable of accounting for all of these features. Our observations collectively indicate that spatial and temporal variations in rainfall patterns, distributed source areas, diverse transport pathways (including tributaries and channel connections), and episodic erosion and sediment incorporation processes interact to initiate scattered processes of mass supplies and thereby surges. These discontinuous materials subsequently result in heterogeneous mass movements that produce the observed fluctuating surge sequences, driven by the spatial and temporal clustering of slope failures, differing sediment mobilization rates, and complex channel transport dynamics. Although many models have been developed to describe debris flow initiation and motion, none have yet captured their sequential characteristics. In the following, we propose a conceptual framework to address this gap.

3.3 Conceptual Framework of Stochastic Model of Surge Generation

The sequential characteristics outlined above motivate the proposal of a stochastic framework to model intermittent surges that originate from source areas and propagate into the main channel within a watershed. We propose that the diversity of surge sequences primarily originates from the spatiotemporal heterogeneity of sources and discontinuous mass processes (e.g., slope failures, bank erosion, sediment assimilation, bed entrainment, and damming-breaching cycles). Field evidence from multiple watersheds definitively demonstrates that slope failures constitute the dominant

https://doi.org/10.5194/egusphere-2026-3226
Preprint. Discussion started: 22 July 2026

initiation mechanism, rather than flow instabilities. This cognition is supported by several factors: (1) consistent spatiotemporal correlation between initial surge arrivals and slope failure events detected by seismic monitoring networks (Lai et al., 2018); (2) volume calculations demonstrating that 85-90 % of surge material derives directly from source-area collapses rather than in-channel erosion (Hungr et al., 2014); and (3) numerical simulations confirming that pure flow instability models cannot reproduce observed surge magnitude distributions without substantial initial mass input from slope failures (Iverson et al., 2016; Pudasaini, 2012). While flow instabilities (e.g., roll waves) may modulate subsequent surge propagation dynamics (Zanuttigh & Lamberti, 2007), they play a secondary role in the initial surge generation process.

The inherent spatiotemporal variability in soil conditions, failure timing, and sediment transport processes motivates our formulation of this system as a stochastic framework. The framework integrates three key components (Fig. 4): (1) Source processes include local rainfall (R_i) and slope failures in the source area (A_i). These failures occur when R_i exceeds critical thresholds. (2) Inter-processes involve bank and bed erosions and channel processes (E_i). These processes depend on the hydrologic conditions and soil-water interactions. In particular, they include: (i) soil liquefaction as the core mechanism for initiation and mobility (Iverson, 1997); (ii) channel erosion as the primary driver of mass amplification (Iverson, 2012); and (iii) granular interactions and phase separation that reorganize internal structure and rheology (Gray & Thornton, 2005). (3) The confluence process links mass supplies from slope failures and inter-processes to the development of surges. This process involves cascading progression from source areas through tributaries to the main channel. These components interact such that tributary flows generate surges only when synchronized with main channel flow. Main channel surges, in turn, require the spatiotemporal alignment of multiple point processes, and the watershed-scale surge sequence emerges from these distributed local contributions. This approach captures the essential randomness while preserving the mechanistic relationships between local-scale processes and emergent surge characteristics.

https://doi.org/10.5194/egusphere-2026-3226
Preprint. Discussion started: 22 July 2026

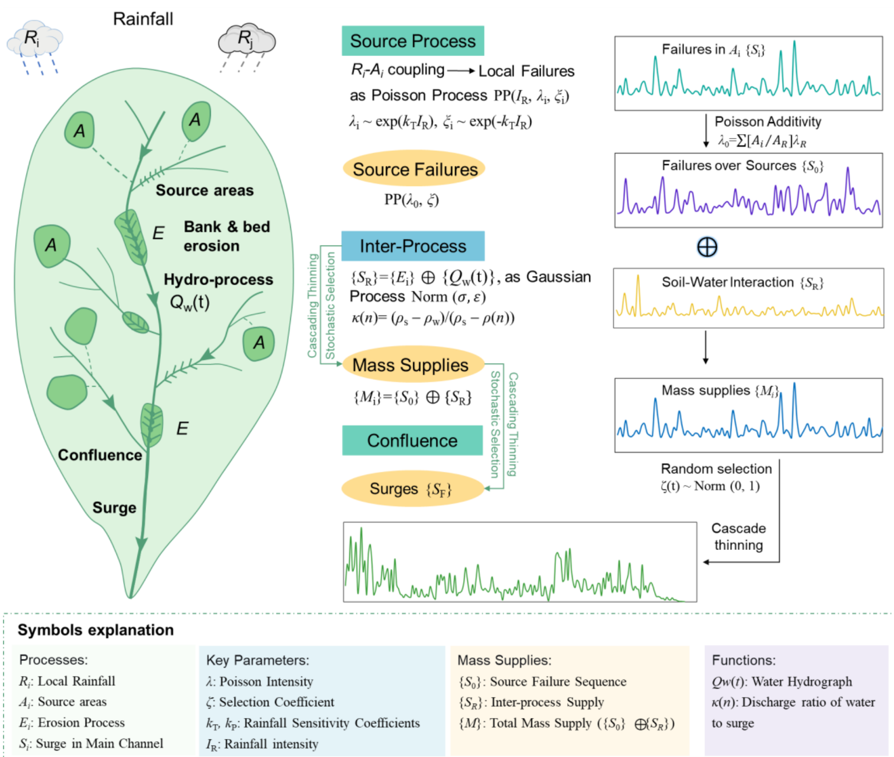

Figure 4. Schematic illustration of surge evolution from source areas to the main channel. Local rainfalls (R_i) initiate slope failures in source areas (A_i), which are further influenced by interrelated erosion processes (E_i), such as bank and streambed erosion, and contribute to hydrograph development ($Q_w(t)$). These processes ultimately converge to form surges in the main channel (S_i).

3.4 Mathematical Formulation

The model comprises three components (Fig. 4): source processes, inter-processes, and confluence. Together, these form the complete scenario of surge evolution, a hierarchical progression from scattered source failures to channeled surges. Mathematically, these include a power-law-based approach to simulate slope failures in the source areas, a Gaussian-distribution selection effect for inter-processes of sediment supplies, and random selective summing to simulate the convergence of multiple sources.

(1) Failures in sources areas

Slope failures in source area A_i induced by rainfall R_i can be formally modeled as a point

https://doi.org/10.5194/egusphere-2026-3226
Preprint. Discussion started: 22 July 2026

process occurring at time t_i and location r_i:

$$\rho(m; r, t) \sim f(m)\delta(r - r_i)\,\delta(t - t_i) \tag{7}$$

where $\delta(x)$ is the Dirac delta function, and $f(m)$ represents the probability density distribution of failure mass m. Field observations and experiments in JJG indicate that the failure mass follows a power-law distribution: $f(m) \sim m^{-\xi}$, while the failure time-interval follows the exponential distribution (i.e., Eq. 5, 6), with the distribution parameters varying with local rainfall intensity under the given soil conditions (Guo et al., 2023). Consequently, the occurrence of failures is described as Poisson process, and the failure sequence $\{S_0\}$ is characterized by a power-law distribution of mass and an exponential distribution of interval ($T(i)$):

$$\{S_0\} = \{S_{T(i)} | T(i) \sim \exp(-\lambda\tau); S_i \sim (m/m_0)^{-\xi}\} \tag{8}$$

where the power-law distribution is normalized using the Pareto distribution (Newman et al., 2005), incorporating a size cutoff m_0 to prevent divergence in the integral. Surge formation can thus be conceptualized as a stochastic selection from the failure sequence $\{S_0\}$, where the mass of each surge originates from slope failures and, by extension, from intermediate erosional processes such as bank and bed scouring occurring during the surge's formation period.

The estimation of total mass contributions from slope failures is supported by the application of power-law distributions, a well-established methodology in landslide inventory analysis (Guzzetti et al., 2002). Field investigations in specific settings, particularly the long observations of debris flow in JJG, have indicated that about 30% of materials from the sources are effectively contributed to the surges. This is consistent to the observations in other regions, e.g., the Oregon Coast Range, where a portion of approximately 20-40% of the initial failure mass contributes to the surge fronts (Iverson et al., 2011). This effective ratio is strongly governed by local terrain conditions, material properties, soil-water interactions, and hydrographic processes, a dependency that has been systematically analyzed in foundational debris-flow studies (Hungr, 2000; Takahashi, 2007). For the present it serves merely as an overall estimation for the magnitude of the potential debris flows, but not as a model parameter.

The power-law failure features a heavy tail, and its variance can be infinite. In such distributions, extreme events occur much more frequently than in Gaussian distributions, and when combined,

https://doi.org/10.5194/egusphere-2026-3226
Preprint. Discussion started: 22 July 2026

they easily generate fluctuations across multiple time scales. This forms the basis for the observed fluctuations in surge sequences. Additionally, intermittent failures, acting as on/off processes, are the primary cause of self-similarity when a large number of these sources are aggregated into surges (Cox, 1984; Embrechts & Maejima, 2002; Willinger et al., 1997).

(2) Inter-processes and hydrographs

The inter-processes linking slope failures to surges involve bank and bed erosion, as well as sediment entrainment within the main channel and its tributaries. These geomorphic processes are primarily governed by hydrological factors, leading to the common assumption that debris-flow discharge equals water discharge multiplied by a constant coefficient, i.e., $Q_f = \kappa Q_w$. However, observations in JJG show that hydrographic processes do not synchronize with the sediment processes; and the linear coefficient $\kappa = (\rho_s - \rho_w)/(\rho_s - \rho)$ is simply describing the material mixture of a flow, which can only be calculated for specific flows and is not a physical metric for measuring the transport capacity of water.

This issue can be further explored through typical events observed in JJG. The surges of two debris flow events (080705 and 130607) do not consistently align temporally with either the recorded rainfall or the hydrographs (Fig. 5). This contrasts with runoff-induced debris flows, where water flow discharge serves as the primary driver for sediment initiation (e.g., Gregoretti et al., 2019).

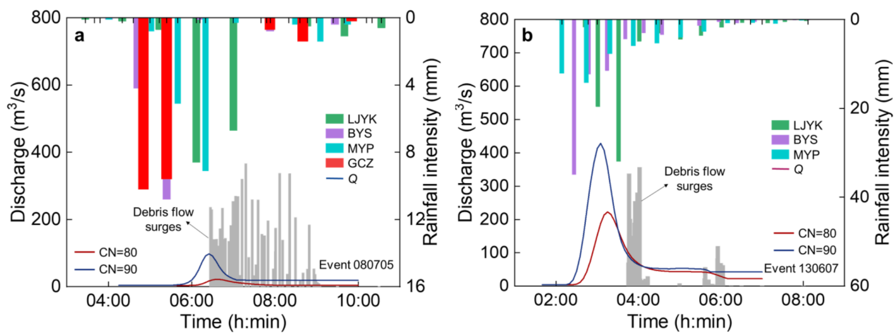

Figure 5. The temporal asynchrony and spatial disparity between sediment surge and hydrograph. (a) rainfall records of different gauges, surge fluctuation, and simulated hydrograph for Event 080705 in JJG; (b) for Event 130607. Hydrographs were simulated by the SCS-CN method using

https://doi.org/10.5194/egusphere-2026-3226
Preprint. Discussion started: 22 July 2026

CN=80 and 90, as usually the case in the watershed (SCS, 1985; Singh & Frevert, 2002).

On the other hand, surges in JJG primarily stem from active source failures — such as those triggered by Coulomb failures — rather than being passively transported by water. As a result, sediment cannot be determined by the hydrographs. Mass movements in sources are discrete, randomly distributed, and follow varied routes (i.e., tributary links), so they as discrete pulse-like supplies to the flow, and the flow discharge can be theoretically expressed as

$$Q_{\mathrm{f}}(t) = Q_{\mathrm{w}}(t) + \sum_{t_i<t} M(t)\delta(t-t_i) \tag{9}$$

in which the mass supplies $M(t)$ is determined by the processes of Eq.7 and 8. As the hydrograph $Q_{\mathrm{w}}(t)$ is unavailable as a temporal process in synch with $M(t)$, we choose to integrate the Q-M mixing as a random process.

Given that κ varies dramatically with surges within a sequence and satisfies the Normal distribution, we reduce the role of hydrograph to a Gaussian process, $N(\sigma, \varepsilon)$, with σ, ε being the mean and variance, respectively, which can be further normalized as a standard distribution $N(0, 1)$, without altering its physical meaning. This formulation integrates the net effect of key hydrological drivers on sediment mobilization: (1) runoff generation, which determines the water discharge (Q_{w}) available for sediment transport and bed erosion (Gregoretti et al., 2019; Kean et al., 2013); (2) pore-pressure diffusion and soil saturation processes, which reduce the effective stress and critical shear stress of channel-bed and bank materials, thereby facilitating sediment entrainment (McCoy et al., 2012); and (3) the spatial and temporal variability of these processes across the watershed (Guo et al., 2023). The assumption of a Gaussian distribution is further supported by the fact that all inter-processes are statistically symmetric — meaning there is no inherent preference for any specific process — and additive in magnitude, with each process contributing to the surge discharge. Consequently, the inter-processes add an extra random component to the failure sequence (Eq. 8), acting as mass supplies, $\{\mathbf{M}\}=\{\mathbf{S_0}\}\oplus\{\mathbf{S_R}\}$, where $\oplus$ denotes the stochastic summation of contributions from multiple sources and processes.

(3) Confluence into surges

https://doi.org/10.5194/egusphere-2026-3226
Preprint. Discussion started: 22 July 2026

Confluence is a cascading process that moves from sources to tributaries and then to the main stream, incorporating both intra-watershed failures and sediment contributions as simplified in the inter-processes. In confluence, hydrological processes play a crucial role in integrating and directing mass supplies from multiple sources. Since failures in source areas and inter-processes occur randomly in space and time, and we focus solely on the final process outcomes — specifically, surge sequences — we simplify these stochastic elements by integrating them with the background hydrograph into a unique aggregating mechanism of mass supplies. This synthesis reduces to a probabilistic selection process representing mass contributions to the surges. Then the hydrological forcing (e.g., runoff scouring capacity, infiltration-induced weakening) on whether and how much a given mass supply (from slope failures or in-channel storage) joins a surge, is integrated into a selection coefficient ζ, which can be simulated by a Gaussian process, based on the Normal distribution of ratio κ. This approach reduces the complex hydrograph-sediment dynamics to a practical random selecting regime.

From sources down to mainstream, the mass supplies will experience cascading selections, i.e., from source sites to tributaries of increasing orders, till the main channel. Formally the cascading processes can be expressed as

$$\boldsymbol{S}_F(j) = \sum_{\Delta T_F(j)} \cdots \sum_{\Delta T_i(j)} \cdots \sum_{\Delta T_0(j)} \zeta(\tau) \boldsymbol{M}(\tau(j)) \tag{10}$$

where $\boldsymbol{M}$ is the mass from $\{\boldsymbol{S}_0\}$, the successive $\Delta T_i\,(j)$ represents the j-th interval in the sequence of the i-th order intermediate processes, and T_F denotes the final interval between surges in the main channel. This cascading operation represents the evolution of mass supply $\{\boldsymbol{M}\}$ from sources into the main channel, involving a series of selection coefficients. This allows one to trace the cascading processes in orders within the framework for the dynamics of water-sediment interactions and the developing of individual surges. However, detailed selection for each step is impractical due to the randomness of inter-processes. Nevertheless, it is ready to be simplified when we solely account for the ultimate surge sequence as entirety. Note that, as mentioned above, both the surges and source failures are identified as Poisson process (PP), the surge developing on watershed scale is simply a transition from PP on sources to PP in channel. Mathematically, this can be reduced to a thinning

https://doi.org/10.5194/egusphere-2026-3226
Preprint. Discussion started: 22 July 2026

from {$\boldsymbol{S}_0$} to {$\boldsymbol{S}_\mathrm{F}$}, i.e.,

$$S_\mathrm{F}(j)=\sum_{\Delta T(j)}\zeta(j)S_0(\tau(j)) \tag{11}$$

where the symbols are the same as in Eq.10. Currently, we consider solely the surge from sources while skipping all the inter-processes. In the selecting summing, the time interval between surges, $\Delta T(j)$ (j=1, 2, …), is generated by exponential distribution as suggested by the Poisson-process nature of surges (Eq. 5). the distribution has typical parameter $\lambda_\mathrm{s} \sim 1/\langle\tau\rangle$, with $\langle\tau\rangle$ the average of interval which is typically on the order of 10^2 seconds.

In this simplification, we employ one single selection coefficient to integrate the cascading collection of mass sources, where the mass supplies occurring within time interval $\Delta T(j)$ are supposed to contribute to the j-th surge, with a selecting factor $\zeta(j)$ at the period, which is generated by a Gaussian process $N(0, 1)$. This assumption is supported by the Central Limit Theorem, which posits that the cumulative effects of multiple independent sub-processes tend to converge toward a normal distribution. Furthermore, this approach prioritizes operational feasibility over detailed mechanistic understanding, a common trade-off in modeling complex systems.

Equation 11 implies that the coefficient not only selects the mass from the source failure sequence but also represents the contribution from inter-process materials, which is accounted as a proportion. Then the mass from source areas and inter-processes are sequentially assembled into successive surges whose magnitudes follow a specific distribution. Equations (7) through (11) collectively describe the mathematical formulation of this mechanism.

3.5 Model Parameters

The framework model outlined above involves the following critical parameters:

Poisson Intensity (λ): The failures over the source areas are characterized by the Poisson intensity $\lambda(A_\mathrm{S}) = \sum(A_i/A_\mathrm{E})\lambda_\mathrm{E}$, where $A_\mathrm{S} = \sum A_i$ represents the total source area, and λ_E is the test intensity of failure to be determined by experiment on a site with area A_E, under a given rainfall intensity. This integrated intensity $\lambda(A_\mathrm{S})$ is mathematically guaranteed by the additivity of the Poisson process (Kingman, 1993). For a source area (A_i) subjected to local rainfall (R_i) with intensity

https://doi.org/10.5194/egusphere-2026-3226
Preprint. Discussion started: 22 July 2026

I_R, experiments indicate that the failures in this area are subjected to the Poisson intensity $\lambda_E \sim \exp(k_T I_R)$ (Guo et al., 2021), where k_T is an empirical coefficient representing the sensitivity of failure rate to rainfall intensity. Then the failures determined by the local R_i-A_i coupling, is extrapolated to the source areas over the watershed.

Pareto Scaling (m_0, ξ): The magnitude cut-off m_0 retains constant for a given rainfall intensity, while the exponent ξ exhibits rainfall sensitivity, following $\xi \sim \exp(-k_P I_R)$, with k_P an empirical coefficient, as supported by experimental findings (Guo et al., 2021).

Selection coefficient (ζ): The selection coefficient ζ is not a conditional factor but rather a functional component modeled as a standard normal variate, $\zeta \sim N(0,1)$, which encapsulates the aggregate influence of unobservable inter-process interactions. By using a normally distributed factor, we integrate the effects of multiple random processes, thereby avoiding the difficulties of explicitly defining the spatiotemporal dynamics of cross-process interactions within the watershed system.

While the processes involved in debris flow formation and evolution are complex and depend on dynamical properties of soils, our framework has minimized the required input data to a core set: (λ, m_0, ξ, ζ). These simplified parameters have distinct physical significance: λ represents the rainfall-source (R_i-A_i) coupling, which depends on the spatial and temporal distribution of rainfall and source areas; m_0 and ξ reflect the intensity and quantity of failures in source areas, respectively. Although both depend on local conditions of rainfall and soils, they possess a certain intrinsic generality and are relatively insensitive to specific event conditions. Finally, ζ integrates the effects of hydrographic processes.

3.6 Model Test

As a stochastic model, it produces a surge sequence rather than individual surges. To validate the simulation results, we employ the Kolmogorov-Smirnov (KS) test, which evaluates the distributional similarity between simulated and observed data. It quantifies the maximum divergence between the empirical cumulative distribution function (ECDF) of the observed data and the theoretical (or reference) cumulative distribution function (CDF) by a distance

https://doi.org/10.5194/egusphere-2026-3226
Preprint. Discussion started: 22 July 2026

$$D = \max\left|S_{\mathrm{m}}(t) - S_{\mathrm{o}}(t)\right| \tag{12}$$

where $S_m(t)$ and $S_o(t)$ are the simulated and observed distribution function, respectively. A smaller D value indicates closer agreement between the observed and simulated distributions.

The critical threshold of D depends on the significant level α, defined as $D_\alpha \sim c(\alpha)/\sqrt{n}$, e.g., $c(0.01) = 1.63$ corresponds to a stringent significance level of $\alpha = 0.01$. This conservative threshold is selected to minimize false negatives, ensuring a robust validation of distributional similarity. The significance of the observed D values was assessed using corresponding p-values, which account for both the sample size and the test statistic (Berger et al., 2014; Zhang et al., 2025). Specifically, $p > 0.05$ indicates that the null hypothesis—that the two samples originate from the same distribution—cannot be rejected at the 5% significance level. Therefore, when this condition is met, the simulation is considered to adequately capture the statistical characteristics of surge sequence. The use of a conservative significance level ($\alpha = 0.01$) ensures high confidence in applications where undetected differences in distribution could have serious implications.

4. Model Operation, Validation, and Application

4.1 Model Realization and Verification in JJG

Now we put the model into operation and use several events with rainfall records as target events to validate the model. The required simulation parameter set, (λ, m_0, ξ, ζ), is listed in Table 1, where the coupling between source area (A_i) and rainfall intensity (R_i) has been estimated using local rainfall intensity (I_R) recorded by each gauge across the area through GIS-based analysis. Given the rainfall-dependent parameters, the failure sequence (Eq. 8) can be simulated, and then the thinning procedure (Eq. 11) can be applied using a set of random selection coefficients (ζ). The resulting mass sequence, $\boldsymbol{S}_F$, which preserves the characteristics of the Poisson process, can be compared to the observed surge sequence.

Table 1 Parameters determining source failures under different rainfalls for events

Events	*R-A* coupling	Poisson intensity	Pareto exponent

https://doi.org/10.5194/egusphere-2026-3226
Preprint. Discussion started: 22 July 2026

	$I_{\text{R-VI}}, A$	$I_{\text{R-II}}, A$	$I_{\text{R-III}}, A$	$I_{\text{R-V}}, A$	$I_{\text{R-IV}}, A$	λ_0	ξ
E080705	-	19.3,12.2	0	19.4, 28.6	18.8, 10.9	195.5	2.00
E990818	6.4, 112.2	12.7, 4.7	-	-	19.5, 80.8	774	2.06
E990716	47, 35.8	2.4, 56.0	-	-	24.7, 63.4	555	2.63
E000704	32, 22.9	21.6,20.9	-	-	37.8, 14.7	245.4	1.57
E080701	-	37.9,16.2	0	25.6, 11.0	37.9, 8.6	178.5	1.86
E030605	32.5, 14.8	22.3, 8.8	-	-	57.8, 12.1	189.9	1.65

The reliability of the proposed model in predicting debris-flow surge sequences was evaluated by examining its capability to replicate key statistical features of observed events—including surge timing, magnitude fluctuations, overall decay trend, and probability distributions. As the model inherently integrates hydrological processes, the assessment focused specifically on comparing simulated and observed sequences of sediment mass (S_F) rather than fluid discharge (Q_f). Simulations were conducted in MATLAB (Zhang et al., 2025), with model performance assessed against three criteria: correspondence in (1) the overall decaying tendency, (2) the timing of decay onset, and (3) the resulting probability distribution P(S) (Eq. 3).

The results demonstrate that the model robustly reproduces the observed surge sequences. For event E030605, the simulated S_F sequence closely aligns with observations, exhibiting a consistent decay trend—initiating at the 31st surge in simulation and the 26th surge in observation (Fig. 6a-2)—and conforming to the same probability distribution (Fig. 6a-3). A similarly close agreement across all criteria was observed for event E080705 (Figures 6b-1 to 6b-3), confirming the model's effectiveness. Additional results are provided in Figure S3 of the Supporting Information.

The simulations confirm that the sequence features can be reproduced by the cascading random processes (Fig. 4). The thinning operation (Eq. 11) effectively transforms the original power-law distribution of mass supplies from failures into Q and S distribution modified by an exponential function (Eq. 3). Additionally, the thinning operation extends the time intervals from order of 10^{-3} s to 10^{2} s, shedding light on the cross-timescale characteristics inherent in debris flow development.

Assessing the validity and accuracy of simulated time series requires a combination of statistical tests, visual inspections, and domain-specific evaluations. Since simulated data rarely align exactly with observed data point by point, and because the model is stochastic in nature, the

https://doi.org/10.5194/egusphere-2026-3226
Preprint. Discussion started: 22 July 2026

focus is on whether the model can reproduce the key statistical properties of the real processes. First, we observe that the predicted magnitude agrees well with the real events (Fig. 6c-1). Next, we compare fundamental descriptive statistics — including the mean, median, standard deviation, range, skewness (3rd moment), and kurtosis (4th moment) — to evaluate central tendency, dispersion, and tail behavior. These metrics provide a baseline assessment of how effectively the simulation reflects the empirical distribution. All metrics are comparable between the simulated and observed data for the representative events (Fig. 6c-2).

Furthermore, the KS test indicates that $D < D_{0.01}$ across all cases, confirming a strong agreement between observed and simulated distributions. This threshold at $\alpha = 0.01$ was chosen to ensure a conservative evaluation and minimize the risk of false negatives. Additionally, the corresponding *p*-values substantially exceed 0.05, providing no statistical basis for rejecting the null hypothesis of distributional similarity (Table S2 in the Supporting Information).

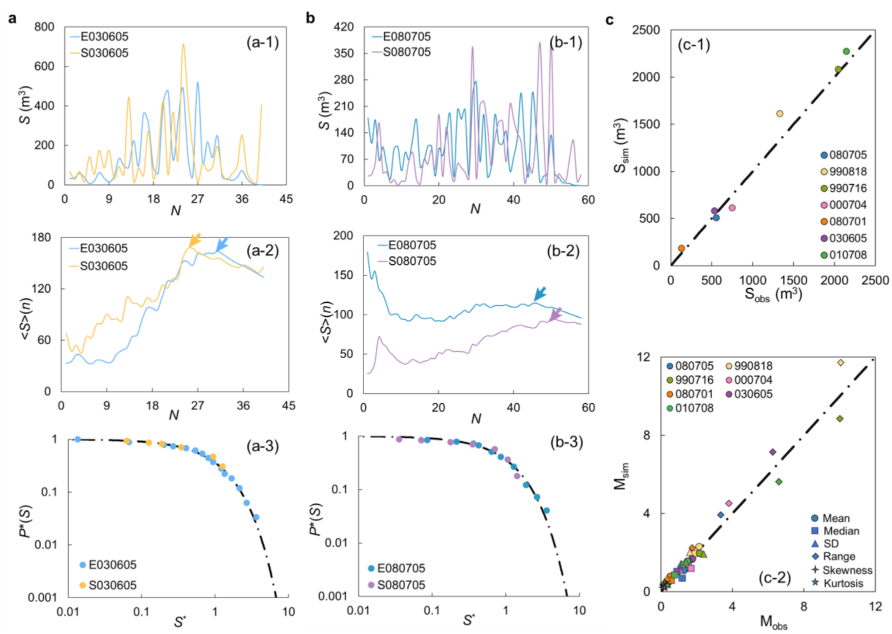

Figure 6. Comparison between simulated and observed surge sequences for two events, E030605 (panel a) and E080705 (panel b) in JJG, along with statistical evaluation of the simulation results (panel c). (a-1) and (b-1) show the sediment fluctuation in the observed and simulated sequences;

https://doi.org/10.5194/egusphere-2026-3226
Preprint. Discussion started: 22 July 2026

(a-2) and (b-2) illustrate the decay trend of $\langle S \rangle_n$ in the observed and simulated sequences; (a-3) and (b-3) present the scaling distribution of sediment volume for the observed and simulated sequences. (c-1) compares sediment volumes between simulated (S_{sim}) and observed (S_{obs}) events. (c-2) compares key statistical parameters: Mean, Median, Standard Deviation (SD), Range, Skewness, and Kurtosis between the simulated (M_{sim}) and observed (M_{obs}) sequences.

4.2 Verification and Generalization of the Model

4.2.1 Statistical Characteristics of Surge Sequences in Global Watershed

The simplification of the model, which ignores the complexities of surge dynamics, allows it to effectively capture the overall statistical characteristics of surge sequences and demonstrates robust applicability across diverse watershed conditions. To assess its generalizability, we conducted comparative analyses with surges in two well-documented sites: Chalk Cliffs (CC) in the United States and Gadria Creek (GC) in Italy (Cavagnaro et al., 2024; Schöffl et al, 2023).

These events have relatively short sequences, containing 10 to 50 surges, yet their statistical properties align closely with those observed in JJG (Figure 7). Notably, $\langle Q \rangle_n$ for these short sequences approaches a near-linear trend rather than a power-law decay (Fig. 6a-1). This suggests the sequence acts as white noise, having strong temporal stochasticity, where the surges are independent and arise from discrete, random inputs (e.g., localized bank or bed erosion) rather than from failures governed by *R-A* coupling. In this sense, the overall decaying trend $\langle Q \rangle_n \sim n^{-q}$ provides an indicator for the forming mechanism of surges.

Since most events involve only a few surges, and some even a single surge, the applicability of sequence-based characteristics appears limited. To enhance generalizability, it is natural to question whether the model applies to single-surge events. For this, we define an "event sequence" as a collection of historical events within a watershed. This event-level sequence spans extended time periods, with intervals ranging from days to months or years. Several event sequences are constructed from debris flows (Fig. 7b, see also Text S1 of the Supporting Information for watershed description and data sources). Notably, these event sequences display the same statistical characteristics as the surge sequences (Fig. 7a-3 & 7b-3).

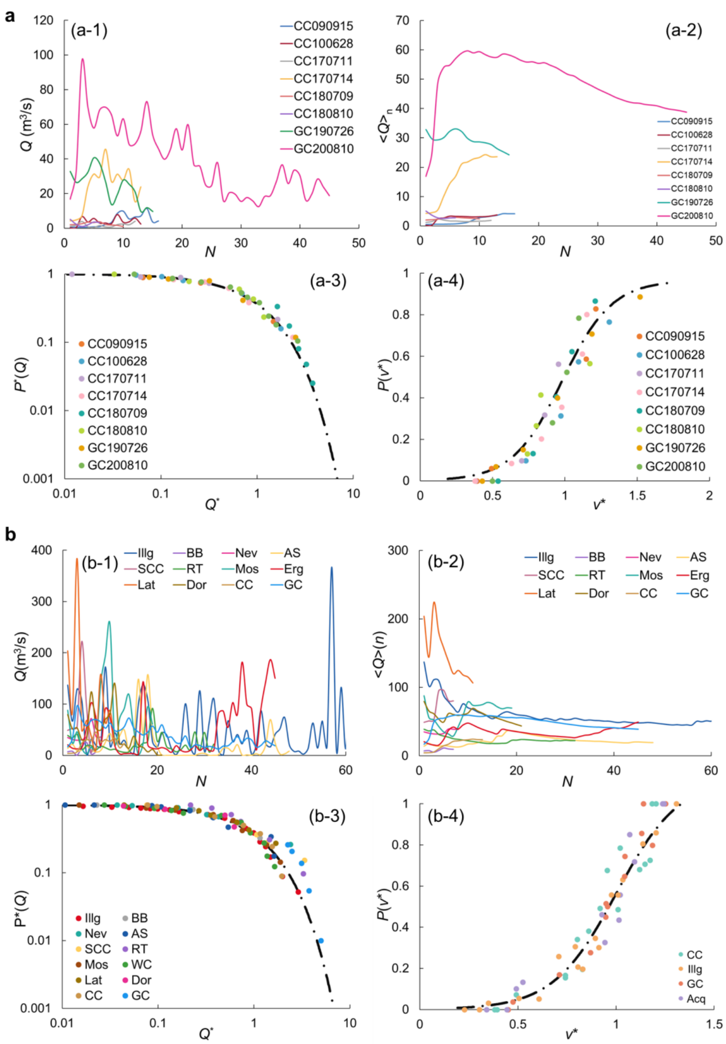

Figure 7. Observed and simulated debris flow surge sequences across global watersheds, demonstrating the same statistical features as the surge sequences. (a) Debris flow events from Chalk Cliffs (CC) and Gadria Creek (GC), with event occurrence times indicated (e.g., 090915 refers to an event on September 15, 2009). (b) Debris flow events from various locations: Illgraben (Illg), Gila National Forest (GNF), Nevada (Nev), Arroyo Seco (AS), Sleeping Child Creek (SCC), Réal Torrent (RT), Moscardo Torrent Basin (Mos), Ergou (Erg), Lattenbach (Lat), Dorfbach (Dor), Chalk Cliffs (CC), and Gadria Creek (GC). (a-1) and (b-1) Q fluctuation; (a-2) and (b-2) general trend of $<Q>_n$; (a-3) and (b-3) Q-distribution; (a-4) and (b-4) v-distribution.

https://doi.org/10.5194/egusphere-2026-3226
Preprint. Discussion started: 22 July 2026

4.2.2 Realization and Verification of Simulation for Global Watersheds

We apply the model to simulate surge sequences for CC and GC using parameters reported in the literature (see Table S5 in the Supporting Information). The simulated sequences (S-CC 170711 and S-GC200810) closely align with the events (E-CC 170711 and E-GC200810), with the same decaying trend of moving average discharge, probability distribution of sediment volume, total sediment volume, and statistical parameters (Fig. 8; see also Fig. S5).

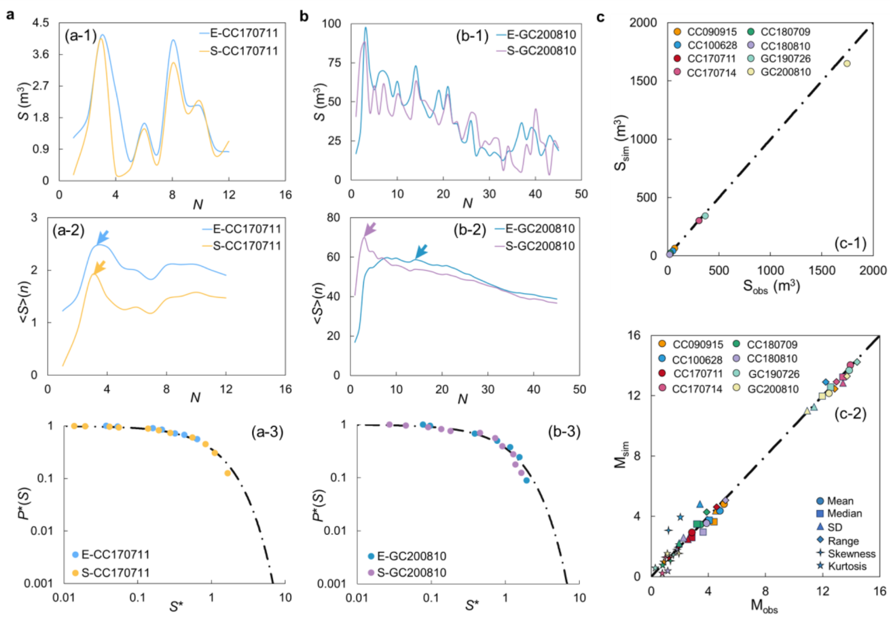

Figure 8. Comparison between simulated and observed surge sequences for two events, CC170711 (panel a) and GC200810 (panel b) in Chalk Cliffs and Gadria Creek, along with statistical evaluation of simulation results for the debris flow sequences (panel c). (a-1) and (b-1) show the sediment fluctuation in the observed and simulated sequences. (a-2) and (b-2) illustrate the $\langle S \rangle_n$ decay trend of the observed (dark colors) and simulated (light colors) sequences. (a-3) and (b-3) present the scaling distribution of sediment for the observed (dark colors) and simulated (light colors) sequences. (c-1) compares sediment volume S between the simulated (S_{sim}) and observed (S_{obs}) sequences. (c-2) compares key statistical parameters (the same as Figure 6c-2) between the simulated (M_{sim}) and observed (M_{obs}) sequences.

Similar to the case of JJG (Fig. 6c, Table S2), we conduct statistical tests on the simulations of

https://doi.org/10.5194/egusphere-2026-3226
Preprint. Discussion started: 22 July 2026

CC and GC, as shown in Figure 8c. The KS results confirm the model's reliability, with all events exhibiting $D<D_{0.01}$ values and corresponding $p>0.05$ (Table S3 in the Supporting Information).

Therefore, the model framework has the capacity to produce the surge sequences only through the information of local rainfall intensity and the coupled source areas in the watershed, without any specific details of the hydrological processes. Practically important is that it may yield the accurate sediment quantity and replicate the probability distributions.

5. Discussions

This study proposes a stochastic framework for modeling the formation and evolution of debris-flow surges, effectively reproducing the statistical characteristics observed in surge sequences. Capturing the characteristics of mass movement from source to mainstream, the model also offers a novel approach for understanding general transport processes in watershed. Several key points warrant further discussion, as they are crucial for enhancing our understanding of debris-flow dynamics and have significant implications for hazard prediction and evaluation.

5.1 Generic Implications of Surge Sequences

The surge sequences exhibit four key characteristics: the high-magnitude fluctuations, an overall decaying trend, a unified probability distribution, and the self-similarity structure. These features provide critical insights into the origins and evolution of debris flows. Notably, the fluctuations of up to three orders of magnitude in Q and S, coupled with the variability in material composition reflected by changes in ρ, cannot be attributed to a single source. While the surge front typically exhibits a high Froude number ($Fr>1$) and thus exists in a supercritical state (Du et al., 2023; Wei et al., 2025), the flow body — especially its watery tails and low-magnitude surges — is subcritical. This dichotomy suggests that the observed diversity of surges is unlikely to stem from flow instability in the form of roll waves (Arai et al., 2013; Berti et al., 1999; Godt & Coe, 2007; Ng & Mei, 1994; Wang et al., 2003). These observations support the hypothesis of multi-source surge generation, wherein the overall decaying trend of Q reflects finite sediment supply — for example, slope failures that stabilize even as rainfall continues. This interpretation is reinforced by the ρ-GSD relationship (Wang et al., 2018; Yang et al., 2019), which distinguishes high-ρ surge

https://doi.org/10.5194/egusphere-2026-3226
Preprint. Discussion started: 22 July 2026

processes — occurring only when flows entrain sufficient coarse material, thereby enhancing sediment transport capacity—from low-ρ surge processes characterized by small-scale finer-grained transport.

The intermittent behavior further highlights discontinuities in sediment supplies form slope failures and bank and bed erosion/assimilation. As both failures and surges are Poisson processes as characterized by exponential distribution of time intervals, the developing of surge is conceptualized as a Poisson transition from point sources to the channel network. This linkage is mathematically represented through a cascading thinning process in our framework (Eq. 10 and 11).

5.2 Essence of the Model

The essence of the model relies in its quantitatively linking local point processes in source areas to the surges on watershed scale. It conceptualizes surges as a thinning of a Poisson process of source failures. This approach abstracts from the complex dynamics of debris flow mobilization and movement, including transitions from landslides (Gabet and Mudd, 2006; Iverson et al., 1997b), channel-bed failures (Gregoretti, 2000), and sediment initiation via the firehose effect (Coe et al., 2008). Within this framework, failures in source areas form a Poisson process, with an intensity correlated to the local rainfall intensity (I_R), while the failure size follows a power-law distribution with exponent ξ. The intermediate erosion and transport processes, coupled to hydrological dynamics, are integrated through a Gaussian selection factor ζ. In essence, the coupling between local rainfall and source area governs the spatial distribution, quantity, mass, and duration of source failures. Thinning the failure sequence represents the randomly aggregation of the mass, thereby regulating the number and timing of surges. The cascading nature of the thinning process, exhibiting both spatial and temporal regularities, inherently supports the self-similarity in surge sequences. Additionally, clustering and fluctuations arise naturally from the underlying stochastic point process.

As a practical model, the parameters have been reduced to the minimum, i.e., (λ, m_0, ξ) (disregarding the selection coefficient ζ generated by Gaussian process). The Poisson intensity (λ) depends on local rainfall and source areas, which are the fundamental data for debris flow surveys and studies (e.g., Gregoretti et al., 2008, 2019); while m_0, ξ, although depending on local

https://doi.org/10.5194/egusphere-2026-3226
Preprint. Discussion started: 22 July 2026

experiments, are following the power-law distribution and fall in a certain range of value and insensitive to predict the statistical features of surge sequences.

A pivotal result of the model is that the thinning operation spontaneously leads to a unified distribution of Q and S (Eq. 3), which transforms the original power-law distribution of failures by multiplying an exponential function as a scaling factor. Consequently, this model reveals a new type of magnitude-frequency correlation emerges, distinct from the power-law distributions commonly observed in natural events such as landslides, floods, and earthquakes (e.g., Bowers et al., 2012; Chang et al., 2020; Croke et al., 2015; Graber et al., 2022; Hergarten, 2002; Marković et al., 2014; Turcotte, 1997). The proposed thinning operation of Poisson process provides the fundamental mechanism underlying the emergence of this novel distribution.

5.3 Insights into Rainfall Thresholds of Debris Flows

The surge phenomena motivates us to revisit the concept of the rainfall thresholds on watershed-level, which currently faces the following difficulties: 1) within a single rainfall event, the intensity, amount, and spatial distribution exhibit substantial variability, it is unrealistic to precisely identify the specific source areas triggered by localized rainfall or to synchronize discrete sediment inputs with a continuous hydrograph; 2) the failures and sediment avalanches as mass supplies are randomly distributed in source areas and channels, making it impossible to use one unique threshold to determine their initiation an on/off; 3) the surge magnitude is usually several orders greater than water discharge, unlikely a linear amplification of the hydrographic process.

To overcome these difficulties, our model addresses the locality of debris flow origins and implicitly uses local critical conditions (via probability) rather than the traditional “rainfall threshold” (e.g., critical discharge or intensity-duration correlation) over a watershed (Gregoretti & Fontana, 2008; Guzzetti et al., 2008; McGuire et al., 2020; Nikolopoulos et al., 2014; Ponziani et al., 2023). Consequently, the model involves critical thresholds at distinct stages: Source failures are governed by parameters (λ and ξ) that depend on local rainfall intensity (I_R); inter-process interactions (e.g., mass movement sustainability) are modeled through stochastic sediment selection governed by ζ; and the surge magnitude is determined by the power-law distribution of failures and the selection coefficient (ζ). This approach acknowledges that debris flow initiation and propagation are governed by interacting thresholds, requiring simultaneous consideration of rainfall intensity, sediment availability, and hydrological connectivity. By decoupling the deterministic "threshold" concept into stage-dependent criteria, as it proves, the model does not predict the occurrences but also account for the spatial and temporal variability of surge sequences.

5.4 Application in Hazard Prediction and Assessment

The model framework provides a probabilistic viewpoint of evaluating debris flows, without requiring data specific to the event details. The involved probability distributions of key parameters (e.g., v, Q, S) (Eq. 2, 3, 4) enable universal tools for hazard evaluation. Notably, the distributions allow direct estimation of flow velocity and individual surge magnitudes. Analysis of data from global events in our study reveals that the distribution parameters for velocity (k, η) and magnitude (μ, M_c) exhibit consistency across diverse watersheds (Fig. 9a, b). Specifically: over 60% of surge velocity fall below 4 ~ 6 m/s ($\eta \approx 5.2 \pm 0.8$), providing statistically robust estimates superior to locally calibrated empirical formulas. Moreover, the clustering of (μ, M_c) near $\mu = 0$ indicates that large-magnitude surges follow exponential distribution, departing from power-law scaling typically employed for describing the magnitude distribution of various disastrous events, such as earthquake, landslide, and flood (e.g., Hergarten, 2002; Turcotte, 1997). Concurrently, surges of small size exhibit large μ values, suggesting that this exponent serves as a meaningful indicator of surge magnitude. The velocity indicator (η) combining with the magnitude indicator (μ) provide the fundamental parameters for hazards assessment and engineering design.

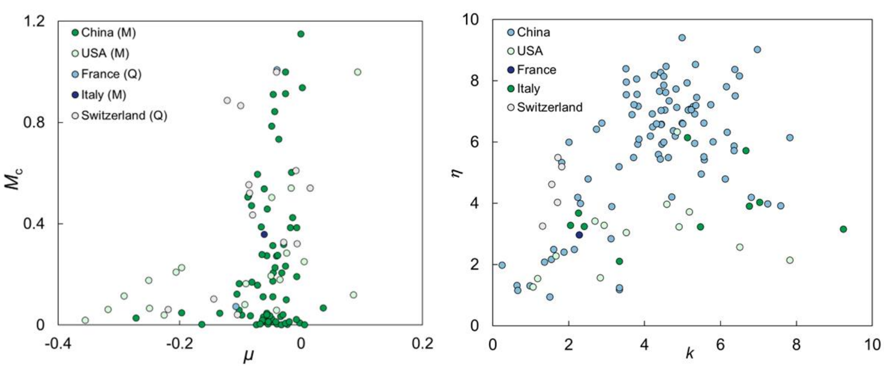

https://doi.org/10.5194/egusphere-2026-3226
Preprint. Discussion started: 22 July 2026

Figure 9. Range of probability distribution parameters for debris-flow surges across global events. (a) Normalized parameters for magnitude (Q or S, and M indicates mixed datasets). (b) Parameters for surge flow velocity.

5.5 Limitations and Perspectives

While the proposed framework effectively captures the macroscopic statistical signatures of surge sequences, its practical application highlights several limitations that warrant further investigation. The first one relies in its specific purpose of capturing the overall statistical features of the surge sequences, which forces ignoring the complex physical processes such as sediment-water interactions, grain-size evolution during transport, and rheological transitions. Its reducing hydrologic action to a Gaussian process integrating the inter-processes might destroy the inherent autocorrelation or long-range correlation between surges; and simplification of the inter-processes further limits its applicability to general cases, such as the debris flows initiated by flood discharges (e.g., Gregoretti et al., 2019). Additionally, the complex inter-processes and the sub-basin morphology, make it hard to determine the cascading selection coefficients, which in turn impedes tracing the GSD evolution in the dynamical processes (Li et al., 2015; Yang et al., 2025; Zhou et al., 2019).

As the limitations arise mainly from the simplification of hydrological processes, the promising perspectives of the model would open when the hydrology-sediment processes are well coupled as to achieve the synchronization at second-timescale (Eq. 9). Then our framework is ready to embrace the dynamical components when the conceptually integrated processes (e.g., the source failures, sediment initiation, and bank erosion) can be timely combined with the hydrographs. Consequently, one would be able to grasp the temporal evolution of soil-water mixture, $Q(t)$ and trace the GSD evolution, as reflected by the ρ-GSD relationship observed in surges (Wang et al., 2018; Yang et al., 2019), as well as the granular effects on the rheology (Yang et a., 2025).

Importantly, the model's ability to trace surges back to their potential sources enables it to predict both how and when such surges will occur. This capability distinguishes it from the traditional dynamical models, which predefine flow properties and rheology based on anticipated conditions without verifying if those conditions actually materialize. Additionally, the ρ-GSD

https://doi.org/10.5194/egusphere-2026-3226
Preprint. Discussion started: 22 July 2026

relationship and the rheology variations dependent on GSD, provide crucial insights into granular effects within flows (Yang et al., 2025), such as the dynamical segregation and sorting of fine and coarse grains. Additionally, hydrological processes as the key line connecting the continuous water flow and the intermittent sediment supplies, as expressed by Eq. 9, may impose inherent temporal coherence between the surges, as characterized by the high Hurst exponent ($H > 0.90$) of the surge sequences (Zhang et al., 2021).

6. Conclusions

The sequential evolution of debris-flow surges encapsulates critical information about the origin and dynamics. However, previous studies on isolated individual surges are focused on the dynamical aspects while ignoring the collective behaviors of sequence as an entirety, such as their fluctuation and general decay trend, the probability distribution of key properties (e.g., velocity, discharge, sediment delivery, and time interval), and the self-similar structures. To fill the gap, we propose a novel conceptual framework to simulate the generation of surge sequences with the observed statistical features, based on a systematical investigation of surge sequences in global watersheds. The following conclusions can be drawn from the model simulations:

(1) A Poisson process is identified for both source-area failures and mainstream surges. The surges are conceptualized as a cascading thinning of the mass sequence originating from failures and intermediate erosional processes. This structure captures the hierarchical evolution across spatial scales, progressing from localized source areas to the main channel.

(2) A Gaussian process is appropriate for the inter-processes of intermittent surge development, which integrates the bank and bed erosions, sediment entrainment, and various soil-water mixing by hydrological processes into a random selection coefficient as a normal variable. This integration reflects the randomness inherent in the processes across scales in watershed.

(3) Site-specific parameters for the model can be easily extrapolated to watershed scale based on local rainfall-related data and the general power-law distribution of source failures. This calibration process enables the model to be effectively applied to any watersheds.

(4) Numerical simulations demonstrate the model’s capacity to replicate observed surge

https://doi.org/10.5194/egusphere-2026-3226
Preprint. Discussion started: 22 July 2026

sequences with remarkable fidelity. A particularly significant outcome is the emergence of a unified probability distribution for discharge and sediment yield, $P(x) = f(\mu)x^{-\mu}\exp(-x/x_c)$, which represents a paradigm shift from conventional power-law-based magnitude-frequency relationships, offering a more nuanced statistical descriptor for debris-flow systems.

Furthermore, this work bridges theoretical stochastic modeling and applied geomorphology, offering a foundational tool for studying earth surface systems characterized by collective event behaviors (Hürlimann et al., 2019; Thouret et al., 2020; Trujillo-Vela et al., 2022). When supported by adequate site-specific data (e.g., rainfall, topography), the framework can significantly enhance hazard prediction through sequence-level modeling, extend to sediment transport in large river basins, and contribute to the planning of preventive engineering measures (Berenguer et al., 2015; Chen et al., 2015).

Appendix A. Notation Symbol Definition

v	velocity of debris flow surge
τ	time interval between successive surges or failures
ρ	flow density of surge
C_s	volumetric solid concentration
Q	debris-flow discharge
$\langle Q\rangle_n$	moving average of discharge
q	exponent of decaying
N_t	turning point for decaying
S	surge sediment volume
$\{S_0\}$	source failure sequence
$\langle S\rangle_n$	moving average of sediment volume
H	Hurst exponent for surge sequence
M_c	characteristic magnitude of surge
η	scale parameter of Weibull distribution
k	shape parameter of Weibull distribution
Fr	Froude number
λ	intensity parameter of Poisson process
R_i	local rainfall
I_R	rainfall intensity

https://doi.org/10.5194/egusphere-2026-3226
Preprint. Discussion started: 22 July 2026

A_i	source area of failures
E_i	channel erosion processes
ξ	exponent of failure power-law distribution
ζ	selection coefficient as a Gaussian variate
$\kappa(n)$	discharge ratio of surge to water
T_F	time interval of the final sequence
D	critical distance in the KS test
α	significance level of KS test

Conflict of Interest

The authors declare no conflicts of interest relevant to this study.

Data Availability Statement

The global debris flow data and MATLAB simulation code are available from the primary repository at https://zenodo.org/records/18743612 (Zhang, 2026). Data for the JJG debris flow site are also available via the Mountain Science Data Center at https://doi.org/10.12380/Debri.msdc.000027 (registration required).

Author contributions

JZ and YL conceived and designed the study. JZ conducted the data analysis, designed and plotted the figures, and wrote the first draft of the manuscript under the supervision of YL. XJG and DRS contributed to the field data collection and laboratory experiments. JMT provided guidance on the methodological framework and contributed to the interpretation of the results. All authors discussed the results, provided critical revisions, and approved the final version of the manuscript.

Acknowledgement

This research is supported by the National Youth Science Foundation (No. 42501091); the NSFC, China (42322703, 42271092); the Open Funds of the Key Laboratory of Mountain Hazards and Engineering Resilience, CAS (No. KLMHER-K22); the China National Postdoctoral Program for Innovation Talent (No. GZC20231347).

References

Arai, M., Huebl, J., and Kaitna, R.: Occurrence conditions of roll waves for three grain–fluid models and comparison with results from experiments and field observation, Geophys. J. Int., 195, 1464-1480, https://doi.org/10.1093/gji/ggt352, 2013.

Arattano, M. and Moia, F.: Monitoring the propagation of a debris flow along a torrent, Hydrol. Sci. J., 44, 811–823, https://doi.org/10.1080/02626669909492275, 1999.

Baggio, T., Mergili, M., and D'Agostino, V.: Advances in the simulation of debris flow erosion: The case study of the Rio Gere (Italy) event of the 4th August 2017, Geomorphology, 381, 107664, https://doi.org/10.1016/j.geomorph.2021.107664, 2021.

Berenguer, M., Sempere-Torres, D., and Hürlimann, M.: Debris-flow forecasting at regional scale by combining susceptibility mapping and radar rainfall, Nat. Hazards Earth Syst. Sci., 15, 587-602, https://doi.org/10.5194/nhess-15-587-2015, 2015.

Berger, V. W. and Zhou, Y.: Kolmogorov–smirnov test: Overview, Wiley statsref: Statistics reference online, https://doi.org/10.1002/9781118445112.stat06558, 2014.

Berti, M., Genevois, R., Simoni, A., and Tecca, P. R.: Field observations of a debris flow event in the Dolomites, Geomorphology, 29, 265-274, https://doi.org/10.1016/S0169-555X(99)00018-5, 1999.

Bolliger, D., Schlunegger, F., and McArdell, B. W.: Comparison of debris flow observations, including fine-sediment grain size and composition and runout model results, at Illgraben, Swiss Alps, Nat. Hazards Earth Syst. Sci., 24, 1035-1049, https://doi.org/10.5194/nhess-24-1035-2024, 2024.

Bowers, M. C., Tung, W. W., and Gao, J. B.: On the distributions of seasonal river flows: lognormal or power law?, Water Resour. Res., 48, W05537, https://doi.org/10.1029/2011WR011308, 2012.

Cannon, S. H., Gartner, J. E., Parrett, C., and Parise, M.: Wildfire-related debris-flow generation through episodic progressive sediment-bulking processes, western USA, in: Debris-Flow Hazards Mitigation: Mechanics, Prediction, and Assessment, edited by: Rickenmann, D. and Chen, C. L., Millpress, Rotterdam, 71-82, 2003.

Cavagnaro, D. B., McCoy, S. W., Kean, J. W., Thomas, M. A., Lindsay, D. N., McArdell, B. W., and Hirschberg, J.: A robust quantitative method to distinguish runoff-generated debris flows from floods, Geophys. Res. Lett., 51, e2024GL109768, https://doi.org/10.1029/2024GL109768, 2024.

Chang, L. C., Chang, F. J., Yang, S. N., Tsai, F. H., Chang, T. H., and Herricks, E. E.: Self-organizing maps of typhoon tracks allow for flood forecasts up to two days in advance, Nat. Commun., 11, 1983, https://doi.org/10.1038/s41467-020-15734-7, 2020.

Chen, X., Cui, P., You, Y., Chen, J., and Li, D.: Engineering measures for debris flow hazard mitigation in the Wenchuan earthquake area, Eng. Geol., 194, 73-85, https://doi.org/10.1016/j.enggeo.2014.10.002, 2015.

Coe, J. A., Kinner, D. A., and Godt, J. W.: Initiation conditions for debris flows generated by runoff at Chalk Cliffs, central Colorado, Geomorphology, 96, 270-297, https://doi.org/10.1016/j.geomorph.2007.03.017, 2008.

Cox, D. R.: Long-range dependence: A Review, in: Statistics: An Appraisal, edited by: David, H. A. and David, H. T., Iowa State University Press, 55–74, 1984.

Croke, J., Denham, R., Thompson, C., and Grove, J.: Evidence of Self-Organized Criticality in riverbank mass failures: a matter of perspective?, Earth Surf. Proc. Land., 40, 953-964, https://doi.org/10.1002/esp.3688, 2015.

Cui, P., Chen, X., Waqng, Y., Hu, K., and Li, Y.: Jiangjia Ravine debris flows in southwestern China, in: Debris-Flow Hazards and Related Phenomena, edited by: Jakob, M. and Hungr, O., Springer, Berlin, 565–594, 2005.

Davies, T. R., Phillips, C. J., Pearce, A. J., and Zhang, X. B.: Debris flow behaviour—an integrated overview, IAHS Publ., 209, 225, 1992.

Du, J., Zhou, G. G., Tang, H., Turowski, J. M., and Cui, K. F.: Classification of stream, hyperconcentrated, and debris flow using dimensional analysis and machine learning, Water Resour. Res., 59, e2022WR033242, https://doi.org/10.1029/2022WR033242, 2023.

Edwards, A. N., Viroulet, S., Johnson, C. G., and Gray, J. M. N. T.: Erosion-deposition dynamics and long distance propagation of granular avalanches, J. Fluid Mech., 915, A9, https://doi.org/10.1017/jfm.2021.34, 2021.

Embrechts, P. and Maejima, M.: Selfsimilar Processes, Princeton University Press, Oxford, Princeton, 2002.

Forterre, Y. and Pouliquen, O.: Long-surface-wave instability in dense granular flows, J. Fluid Mech., 486, 21-50, https://doi.org/10.1017/S0022112003004555, 2003.

Fryirs, K.: (Dis)Connectivity in catchment sediment cascades: a fresh look at the sediment delivery problem, Earth Surf. Proc. Land., 38, 30-46, https://doi.org/10.1002/esp.3242, 2013.

Gabet, E. J. and Mudd, S. M.: The mobilization of debris flows from shallow landslides, Geomorphology, 74, 207-218, https://doi.org/10.1016/j.geomorph.2005.08.013, 2006.

Godt, J. W. and Coe, J. A.: Alpine debris flows triggered by a 28 July 1999 thunderstorm in the central Front Range, Colorado, Geomorphology, 84, 80–97, https://doi.org/10.1016/j.geomorph.2006.07.009, 2007.

Graber, A. and Santi, P.: Power law models for rockfall frequency-magnitude distributions: review and identification of factors that influence the scaling exponent, Geomorphology, 418, 108463, https://doi.org/10.1016/j.geomorph.2022.108463, 2022.

https://doi.org/10.5194/egusphere-2026-3226
Preprint. Discussion started: 22 July 2026

Gray, J. M. N. T. and Thornton, A. R.: A theory for particle size segregation in shallow granular free-surface flows, P. Roy. Soc. A-Math. Phy., 461, 1447-1473, https://doi.org/10.1098/rspa.2004.1420, 2005.

Gregoretti, C.: The initiation of debris flow at high slopes: experimental results, J. Hydraul. Res., 38, 83-88, https://doi.org/10.1080/00221680009498343, 2000.

Gregoretti, C. and Fontana, G. D.: The triggering of debris flow due to channel-bed failure in some alpine headwater basins of the Dolomites: Analyses of critical runoff, Hydrol. Process., 22, 2248-2263, https://doi.org/10.1002/hyp.6821, 2008.

Gregoretti, C., Stancanelli, L. M., Bernard, M., Boreggio, M., Degetto, M., and Lanzoni, S.: Relevance of erosion processes when modelling in-channel gravel debris flows for efficient hazard assessment, J. Hydrol., 568, 575-591, https://doi.org/10.1016/j.jhydrol.2018.10.001, 2019.

Guo, X., Li, Y., Yao, Y., Liu, D., and Zhang, J.: A pareto–Poisson process model for intermittent debris flow surges developing from slope failures, Eng. Geol., 314, 106998, https://doi.org/10.1016/j.enggeo.2023.106998, 2023.

Guo, X. J., Li, Y., Cui, P., Yan, Y., Wang, B. L., and Zhang, J.: Spatiotemporal characteristics of discontinuous soil failures on debris flow source slopes, Eng. Geol., 295, 106438, https://doi.org/10.1016/j.enggeo.2021.106438, 2021.

Guzzetti, F., Malamud, B. D., Turcotte, D. L., and Reichenbach, P.: Power-law correlations of landslide areas in central Italy, Earth Planet. Sc. Lett., 195, 169-183, https://doi.org/10.1016/s0012-821x(01)00589-1, 2002.

Guzzetti, F., Peruccacci, S., Rossi, M., and Stark, C. P.: The rainfall intensity–duration control of shallow landslides and debris flows: an update, Landslides, 5, 3-17, https://doi.org/10.1007/s10346-007-0112-1, 2008.

Hergarten, S.: Self-Organized Criticality in Earth Systems, Springer, Berlin, 2002.

Hong, Y., Wang, J. P., Li, D. Q., Cao, Z. J., Ng, C. W. W., and Cui, P.: Statistical and probabilistic analyses of impact pressure and discharge of debris flow from 139 events during 1961 and 2000 at Jiangjia Ravine, China, Eng. Geol., 187, 122-134, https://doi.org/10.1016/j.enggeo.2014.12.011, 2015.

Hu, K., Wei, F., and Li, Y.: Real-time measurement and preliminary analysis of debris-flow impact force at Jiangjia Ravine, China, Earth Surf. Proc. Land., 36, 1268-1278, https://doi.org/10.1002/esp.2155, 2011.

Hungr, O.: Analysis of debris flow surges using the theory of uniformly progressive flow, Earth Surf. Proc. Land., 25, 483-495, https://doi.org/10.1002/(SICI)1096-9837(200005)25:5<483::AID-ESP76>3.0.CO;2-Z, 2000.

Hungr, O., Leroueil, S., and Picarelli, L.: The Varnes classification of landslide types, an update,

https://doi.org/10.5194/egusphere-2026-3226
Preprint. Discussion started: 22 July 2026

Landslides, 11, 167-194, https://doi.org/10.1007/s10346-013-0436-y, 2014.

Hürlimann, M., Coviello, V., Bel, C., Guo, X., Berti, M., Graf, C., and Yin, H. Y.: Debris-flow monitoring and warning: Review and examples, Earth-Sci. Rev., 199, 102981, https://doi.org/10.1016/j.earscirev.2019.102981, 2019.

Iverson, R. M.: Hydraulic modeling of unsteady debris-flow surges with solid-fluid interactions, in: Debris-Flow Hazards Mitigation: Mechanics, Prediction and Assessment, edited by: Chen, C.-L., Am. Soc. of Civ. Eng., Reston, Va., 550–560, 1997a.

Iverson, R. M.: The physics of debris flows, Rev. Geophys., 35, 245-296, https://doi.org/10.1029/97RG00426, 1997b.

Iverson, R. M.: Elementary theory of bed-sediment entrainment by debris flows and avalanches, J. Geophys. Res.-Earth, 117, F03006, https://doi.org/10.1029/2011jf002189, 2012.

Iverson, R. M.: Debris flows: behaviour and hazard assessment, Geology Today, 30, 15-20, https://doi.org/10.1111/gto.12037, 2014.

Iverson, R. M., Reid, M. E., and LaHusen, R. G.: Debris-flow mobilization from landslides, Annu. Rev. Earth Pl. Sc., 25, 85-138, https://doi.org/10.1146/annurev.earth.25.1.85, 1997.

Iverson, R. M., Reid, M. E., Logan, M., LaHusen, R. G., Godt, J. W., and Griswold, J. P.: Positive feedback and momentum growth during debris-flow entrainment of wet bed sediment, Nat. Geosci., 4, 116-121, https://doi.org/10.1038/ngeo1040, 2011.

Iverson, R. M., George, D. L., and Logan, M.: Debris flow runup on vertical barriers and adverse slopes, J. Geophys. Res.-Earth, 121, 2333-2357, https://doi.org/10.1002/2016jf003933, 2016.

Kean, J. W., Staley, D. M., and Cannon, S. H.: In situ measurements of post-fire debris flows in southern California: Comparisons of the timing and magnitude of 24 debris-flow events with rainfall and soil moisture conditions, J. Geophys. Res.-Earth, 116, F04019, https://doi.org/10.1029/2011JF002005, 2011.

Kean, J. W., McCoy, S. W., Tucker, G. E., Staley, D. M., and Coe, J. A.: Runoff-generated debris flows: Observations and modeling of surge initiation, magnitude, and frequency, J. Geophys. Res.-Earth, 118, 2190-2207, https://doi.org/10.1002/jgrf.20148, 2013.

Kingman, J. F. C.: Poisson Processes, Oxford Studies in Probability 3, Oxford University Press Inc., New York, 1993.

Krishnan, V.: Probability and Random Processes, John Wiley & Sons, 2015.

Lai, V. H., Tsai, V. C., Lamb, M. P., Ulizio, T. P., and Beer, A. R.: The seismic signature of debris flows: Flow mechanics and early warning at Montecito, California, Geophys. Res. Lett., 45, 5528-5535, https://doi.org/10.1029/2018GL077683, 2018.

Lari, S., Frattini, P., and Crosta, G. B.: A probabilistic approach for landslide hazard analysis, Eng. Geol., 182, 3-14, https://doi.org/10.1016/j.enggeo.2014.07.015, 2014.

Li, Y., Liu, J., Su, F., Xie, J., and Wang, B.: Relationship between grain composition and debris flow characteristics: a case study of the Jiangjia Gully in China, Landslides, 12, 19-28,

https://doi.org/10.5194/egusphere-2026-3226
Preprint. Discussion started: 22 July 2026

https://doi.org/10.1007/s10346-014-0475-z, 2015a.

Li, Y., Wang, B. L., Zhou, X. J., and Gou, W. C.: Variation in grain size distribution in debris flow, J. Mt. Sci.-Engl., 12, 682-688, https://doi.org/10.1007/s11629-014-3351-3, 2015b.

Liu, J., Li, Y., Su, P., Cheng, Z., and Cui, P.: Temporal variation of intermittent surges of debris flow, J. Hydrol., 365, 322-328, https://doi.org/10.1016/j.jhydrol.2008.12.005, 2009.

Liu, X., Wang, F., Nawnit, K., Lv, X., and Wang, S.: Experimental study on debris flow initiation, B. Eng. Geol. Environ., 79, 1565-1580, https://doi.org/10.1007/s10064-019-01618-8, 2020.

Marković, D. and Gros, C.: Power laws and self-organized criticality in theory and nature, Phys. Rep., 536, 41-74, https://doi.org/10.1016/j.physrep.2013.11.002, 2014.

McCoy, S. W., Kean, J. W., Coe, J. A., Tucker, G. E., Staley, D. M., and Wasklewicz, T. A.: Sediment entrainment by debris flows: In situ measurements from the headwaters of a steep catchment, J. Geophys. Res.-Earth, 117, F03016, https://doi.org/10.1029/2011jf002278, 2012.

McGuire, L. A. and Youberg, A. M.: What drives spatial variability in rainfall intensity-duration thresholds for post-wildfire debris flows? Insights from the 2018 Buzzard Fire, NM, USA, Landslides, 17, 2385-2399, https://doi.org/10.1007/s10346-020-01470-y, 2020.

Mitchell, A., Zubrycky, S., McDougall, S., Aaron, J., Jacquemart, M., Hübl, J., and Graf, C.: Variable hydrograph inputs for a numerical debris-flow runout model, Nat. Hazards Earth Syst. Sci., 22, 1627-1654, https://doi.org/10.5194/nhess-2021-352, 2022.

Nagl, G., Hübl, J., and Scheidl, C.: Real-scale measurements of debris-flow run-ups, Landslides, 21, 963-973, https://doi.org/10.1007/s10346-023-02204-6, 2024.

Newman, M. E. J.: Power laws, Pareto distributions and Zipf's law, Contemp. Phys., 46, 323-351, http://dx.doi.org/10.1080/00107510500052444, 2005.

Ng, C. O. and Mei, C. C.: Roll waves on a shallow layer of mud modelled as a power-law fluid, J. Fluid Mech., 263, 151-184, https://doi.org/10.1017/s0022112094004064, 1994.

Nikolopoulos, E. I., Crema, S., Marchi, L., Marra, F., Guzzetti, F., and Borga, M.: Impact of uncertainty in rainfall estimation on the identification of rainfall thresholds for debris flow occurrence, Geomorphology, 221, 286-297, https://doi.org/10.1016/j.geomorph.2014.06.015, 2014.

Ponziani, M., Ponziani, D., Giorgi, A., Stevenin, H., and Ratto, S. M.: The use of machine learning techniques for a predictive model of debris flows triggered by short intense rainfall, Nat. Hazards, 117, 143-162, https://doi.org/10.1007/s11069-023-05853-x, 2023.

Pudasaini, S. P.: A general two-phase debris flow model, J. Geophys. Res.-Earth, 117, F03010, https://doi.org/10.1029/2011JF002186, 2012.

Schöffl, T., Nagl, G., Koschuch, R., Schreiber, H., Hübl, J., and Kaitna, R.: A Perspective of Surge Dynamics in Natural Debris Flows Through Pulse-Doppler Radar Observations, J. Geophys. Res.-Earth, 128, e2023JF007171, https://doi.org/10.1029/2023JF007171, 2023.

SCS: Hydrology, National Engineering Handbook, Soil Conservation Service, USDA, Washington, DC, 1985.

Simoni, A., Bernard, M., Berti, M., Boreggio, M., Lanzoni, S., Stancanelli, L. M., and Gregoretti, C.: Runoff-generated debris flows: Observation of initiation conditions and erosion–deposition dynamics along the channel at Cancia (eastern Italian Alps), Earth Surf. Proc. Land., 45, 3556-3571, https://doi.org/10.1002/esp.4981, 2020.

Singh, V. P. and Frevert, D. K. (Eds.): Mathematical models of small watershed hydrology and applications, Water Resources Publication, 2002.

Stone, G. C. and Van Heeswijk, R. G.: Parameter estimation for the Weibull distribution, IEEE T. Electr. Insul., EI-12, 253-261, https://doi.org/10.15170/szigma.55.1249, 2007.

Takahashi, T.: Debris flow, IAHR Monograph Series, Balkema, Rotterdam, 1991.

Takahashi, T.: Debris flow: mechanics, prediction and countermeasures, Taylor & Francis, https://doi.org/10.1201/9780203946282, 2007.

Thouret, J. C., Antoine, S., Magill, C., and Ollier, C.: Lahars and debris flows: Characteristics and impacts, Earth-Sci. Rev., 201, 103003, https://doi.org/10.1016/j.earscirev.2019.103003, 2020.

Trujillo-Vela, M. G., Ramos-Cañón, A. M., Escobar-Vargas, J. A., and Galindo-Torres, S. A.: An overview of debris-flow mathematical modelling, Earth-Sci. Rev., 232, 104135, https://doi.org/10.1016/j.earscirev.2022.104135, 2022.

Turcotte, D. L.: Fractals and Chaos in Geology and Geophysics, Cambridge University Press, Cambridge, New York, Melbourne, https://doi.org/10.5860/choice.30-2691, 1997.

Viroulet, S., Edwards, A. N., Johnson, C. G., Kokelaar, B. P., and Gray, J. M. N. T.: Shedding dynamics and mass exchange by dry granular waves flowing over erodible beds, Earth Planet. Sc. Lett., 523, 115700, https://doi.org/10.1016/j.epsl.2019.07.003, 2019.

Wang, B. L., Li, Y., Liu, D. C., and Liu, J. J.: Debris flow density determined by grain composition, Landslides, 15, 1205-1213, https://doi.org/10.1007/s10346-017-0912-x, 2018.

Wang, G., Sassa, K., and Fukuoka, H.: Downslope volume enlargement of a debris slide–debris flow in the 1999 Hiroshima, Japan, rainstorm, Eng. Geol., 69, 309-330, https://doi.org/10.1016/s0013-7952(02)00289-2, 2003.

Wei, L., Song, D., Cui, P., Su, L., Zhou, G. G., Hu, K., and Tang, H.: A long-term dataset of debris-flow and hydrometeorological observations from 1961 to 2024 at Jiangjia Ravine, China, Earth Syst. Sci. Data Discuss., 2025, 1-35, https://doi.org/10.5194/essd-2025-190, 2025.

Willinger, W., Taqqu, M. S., Sherman, R., and Wilson, D. V.: Self-similarity through high-variability: statistical analysis of Ethernet LAN Traffic at the source level, IEEE/ACM T. Network., 5, 71–86, 1997.

Yang, T., Li, Y., Zhang, Q., and Jiang, Y.: Calculating debris flow density based on grain-size distribution, Landslides, 16, 515-522, https://doi.org/10.1007/s10346-018-01130-2, 2019.

https://doi.org/10.5194/egusphere-2026-3226
Preprint. Discussion started: 22 July 2026

Yang, T., Li, Y., Guo, X., Cheng, W., Zhong, Q., Liu, J., and Luo, J.: Changes in granular textures of debris flow viewed from the unified grain size distribution, Nat. Hazards, 121, 12817-12836, https://doi.org/10.1007/s11069-025-07297-x, 2025a.

Yang, T., Li, Y., Guo, X., Wang, K., Zhang, J., Luo, J., and Liu, J.: Rheology of debris flows: Insights from experiments with coarse-grained matrix, Earth Surf. Proc. Land., 50, e6069, https://doi.org/10.1002/esp.6069, 2025b.

Yong, L., Jingjing, L., Kaiheng, H., and Pengcheng, S.: Probability distribution of measured debris-flow velocity in Jiangjia Gully, Yunnan Province, China, Nat. Hazards, 60, 689-701, https://doi.org/10.1007/s11069-011-0033-0, 2012.

Yong, L., Xiaojun, Z., Pengcheng, S., Yingde, K., and Jingjing, L.: A scaling distribution for grain composition of debris flow, Geomorphology, 192, 30-42, https://doi.org/10.1016/j.geomorph.2013.03.015, 2013.

Zanuttigh, B. and Lamberti, A.: Numerical modelling of debris surges based on shallow-water and homogeneous material approximations, J. Hydraul. Res., 42, 376–389, https://doi.org/10.1080/00221686.2004.9728403, 2004.

Zanuttigh, B. and Lamberti, A.: Instability and surge development in debris flows, Rev. Geophys., 45, RG3006, https://doi.org/10.1029/2005RG000175, 2007.

Zhang, J.: Worldwide Debris-Flow Dataset and Pareto-Poisson Simulation Code, Zenodo [data set], https://doi.org/10.5281/zenodo.18743612, 2026.

Zhang, J., Li, Y., Guo, X., Yang, T., Liu, D., and Yu, B.: Temporal characteristics of debris flow surges, Front. Earth Sci., 9, 660655, https://doi.org/10.5194/egusphere-egu22-3302, 2021.

Zhang, J., Li, Y., Cui, Y., Wu, Z., Xue, Y., Cheng, J., and Luo, A.: Unity of terrestrial and extraterrestrial soils in granular configuration, Earth Planet. Sc. Lett., 654, 119239, https://doi.org/10.1016/j.epsl.2025.119239, 2025.

Zhang Jun and Li Yong: Data on 95 Debris Flows from Jiangjiagou (1987-2017), Mountain Science Data Center, https://doi.org/10.12380/Debri.msdc.000027, 2025.

Zhou, G. G., Li, S., Song, D., Choi, C. E., and Chen, X.: Depositional mechanisms and morphology of debris flow: physical modelling, Landslides, 16, 315-332, https://doi.org/10.1007/s10346-018-1095-9, 2019.